

# Backward elastic $pd$ scattering at intermediate energies

Yu. N. Uzikov

*Joint Institute for Nuclear Research, Dubna*

Fiz. Élem. Chastits At. Yadra **29**, 1405–1455 (November–December 1998)

The theoretical approaches to the description of backward elastic  $pd$  scattering at energies 0.5–2 GeV are reviewed. In addition to the mechanisms of neutron exchange and single  $pN$  scattering, the role of  $N^*$ -isobar exchange is studied using the six-quark model for the  $dNN^*$  vertex. Relativistic effects are taken into account within the Hamiltonian dynamics of systems with a fixed number of particles. The important role of Glauber rescatterings in the initial and final states in the neutron-transfer mechanism is displayed. Special attention is paid to the mechanism of  $\Delta$ -isobar excitation, which, despite the large momentum transfer, is rather weakly sensitive to the high-momentum components of the deuteron wave function and dominates at incident proton energies  $T_p = 0.5$ –1 GeV. The reaction  $pp \rightarrow pn\pi^+$  is studied in the  $\Delta$ -resonance region in order to determine the parameters of the amplitudes for  $NN \leftrightarrow N\Delta$  transitions needed to calculate the  $\Delta$ -isobar contribution to the process  $pd \rightarrow dp$ . It is shown that the amplitude of the  $\Delta$ -resonance mechanism for the process  $pd \rightarrow dp$  is very sensitive to the parameters of the  $\pi NN$ ,  $\pi N\Delta$ ,  $\rho NN$ , and  $\rho N\Delta$  vertex form factors. The role of more exotic mechanisms is briefly discussed. © 1998 American Institute of Physics. [S1063-7796(98)00306-4]

## 1. INTRODUCTION

Interest in the study, both theoretical<sup>1–15</sup> and experimental,<sup>16–23</sup> of backward elastic  $pd$  scattering at energies  $\sim 1$ –2 GeV has not abated in the last 30 years, mainly because, owing to the large momentum transfer, this is one of the simplest processes in which information about the properties of the  $NN$  interaction in the nucleon overlap region can be extracted. In this process the deuteron makes use of its ability to accept, as a single object, a large momentum and energy transfer a hundred times greater than its binding energy. The question of to what degree this property of the deuteron may be related to the 6-quark and relativistic structure of its wave function is being investigated systematically in theoretical studies. Information important for determining the mechanism of backward elastic  $pd$  scattering,  $pd \rightarrow dp$ , can be obtained by measuring the corresponding complete set of independent polarization observables in collinear kinematics. There are plans to do this at the JINR.<sup>22</sup>

The active study of backward elastic  $pd$  scattering over the last few decades has led to a number of interesting ideas in intermediate-energy physics such as the existence in nuclei of nucleon isobars<sup>1</sup>  $N^*$  and three-baryon resonances,<sup>8</sup> the important role of virtual pions,<sup>2,3</sup> and the question of the color dynamics in this process.<sup>10</sup> However, the results of these studies have not convincingly shown that the mechanisms most sensitive to the high-momentum components of the deuteron wave function, i.e., nucleon exchange (NE) and single scattering (SS), play the principal role in the process  $pd \rightarrow dp$  at energies  $T_p \geq 0.5$  GeV. The statements made in the literature that the SS (Ref. 7) or NE (Ref. 11) mechanism dominates are based on rather artificial assumptions about the elastic form factor at large momentum transfers  $Q \geq 2$  GeV/c or high-momentum components of the wave

function, respectively. On the contrary, when better-justified, so-called realistic deuteron wave functions are used, calculations<sup>4</sup> show that the NE mechanism is suppressed owing to distortions in the initial and final states, and so the absolute value of the observed cross section in the energy range  $\sim 0.5$ –2 GeV is clearly underestimated. Moreover, advances in polarization measurements<sup>19,21</sup> have revealed a sharp contradiction between the predictions of the NE mechanism and the experimental data for the tensor polarization  $t_{20}$ . The calculations of Ref. 9 performed using the fully covariant Bethe–Salpeter formalism for the pole mechanism of NE did not lead to improved agreement with experiment. On the other hand, it became clear that at certain energies there can be a large momentum transfer owing to mechanisms which do not require the extensive involvement of the high-momentum components of the nuclear wave function. One such mechanism is double  $pN$  scattering with  $\Delta$ -isobar excitation in the process  $pd \rightarrow dp$ , which dominates at initial energies in the range 0.5–1.0 GeV. Using the  $\Delta$ -resonance mechanism, it is possible to obtain a qualitative explanation of the observed absolute value of the cross section for  $T_p = 0.5$ –1 GeV (Refs. 12 and 13), and, according to Ref. 12, also of the tensor polarization  $t_{20}$ . For  $T_p \geq 1$  GeV, the excitation of heavier nucleon isobars  $N^*$  might play a similar role.

Nevertheless, at present it cannot be stated that the question of the role and, even more so, of the absolute value of the contribution of the NE mechanism to the process  $pd \rightarrow dp$  has been definitively answered. First, there is no unambiguous, model-independent information about the high-momentum components of the deuteron wave function in the  $pn$  sector. Second, disagreement with experiment regarding  $t_{20}$  has been the result of all earlier calculations

based on the NE mechanism (a) neglecting the initial- and final-state interactions and (b) neglecting  $N^*$ -isobar exchange, of which the most important for obtaining agreement with experiment regarding  $t_{20}$  is expected to be the  $P$ -wave contribution at the  $dNN^*$  vertex. The important role of these effects was recently pointed out in Ref. 24, according to which the experimental data on both the differential cross section and  $t_{20}$  in the inclusive reaction  $d+A \rightarrow p(0^\circ)+X$  (Ref. 25) can be described using the NE mechanism with realistic deuteron wave functions if the contribution of  $N^*$  exchange and rescattering in the initial and final states is taken into account. In view of the nontrivial correlation (see, for example, Ref. 26) observed between the experimental data on deuteron disintegration<sup>25</sup>  $d+A \rightarrow p(0^\circ)+X$ , on the one hand, and backward elastic  $pd$  scattering, on the other, there are grounds for believing that a similar result might be obtained regarding the role of neutron and  $N^*$ -isobar exchange in the process  $pd \rightarrow dp$ . Third, it should be stressed that the conclusion<sup>4</sup> that distortions tend to play a suppressive role in the process  $pd \rightarrow dp$  was arrived at on the basis of a rather formal method without any qualitative explanation of the results obtained. This method has not been applied to backward proton scattering on more complex nuclei. The role of rescatterings in the process  $pd \rightarrow dp$  was later studied<sup>7</sup> using the eikonal approximation, but with a purely nonrelativistic treatment of the NE mechanism, which significantly decreases its contribution. It has recently been shown<sup>27</sup> that Glauber rescatterings play a very important role in backward elastic  $p\ ^3\text{He}$  scattering within the mechanism of  $np$ -pair exchange. It was shown that rescatterings lead to significant (by a factor of  $\sim 30$ – $40$ ) suppression of the absolute value of the cross section for  $p\ ^3\text{He}$  scattering at  $\theta_{\text{c.m.}} = 180^\circ$ . As a result, it was possible to obtain a satisfactory description of the absolute value of the cross section in the energy range  $T_p = 0.9$ – $1.7$  GeV and, simultaneously, the shape of the angular distribution, without any free parameters. Of course, it is interesting to apply this method to the description of backward elastic  $pd$  scattering using the NE mechanism, as done recently in Ref. 28. Along with neutron exchange, there we studied  $N^*$ -isobar exchange using the same model for the  $dNN^*$  vertex as in Ref. 24, and, in addition, we included rescatterings in the initial and final states using the method of Ref. 27. Significant improvements in the application of the  $6q$  model to the process  $pd \rightarrow dp$  were made in Ref. 29.

Here, in discussing the results obtained in recent years in theoretical studies of the process  $pd \rightarrow dp$ , we shall focus equally on mechanisms sensitive to the high-momentum components of the deuteron wave function and mechanisms which hinder the extraction of this information, and also the interference between them.

## 2. THE RELATIVISTIC DYNAMICS OF COMPOSITE SYSTEMS

In processes involving bound systems  $\{\alpha\beta\}$ , where  $\alpha$  and  $\beta$  are two constituents of mass  $m_\alpha$  and  $m_\beta$  and  $\{\alpha\beta\}$  is their bound state of mass  $M_{\{\alpha\beta\}}$ , with  $M_{\{\alpha\beta\}} < m_\alpha + m_\beta$ , relativistic dynamics effects become important at constituent

momentum comparable to the rest mass:  $|\mathbf{q}_\alpha| \sim m_\alpha$ ,  $|\mathbf{q}_\beta| \sim m_\beta$ . This is completely obvious from the viewpoint of the kinematical relation between the mass, momentum, and total energy of a particle  $E = \sqrt{m^2 + \mathbf{q}^2}$ , but the deep origin of these relativistic effects is dynamical, i.e., it is related to the interaction at nonzero (or even arbitrarily small) values of the binding energy  $\varepsilon = m_\alpha + m_\beta - M_{\{\alpha\beta\}}$ . At a binding energy comparable to the constituent rest mass, for example in the amplitudes of the transitions  $d \rightarrow \Delta + \Delta$  and  $d \rightarrow N + N^*$ , relativistic effects must be included even at zero constituent momentum  $\mathbf{q}_\alpha \sim 0$ . This fact is not well known in the literature (see Ref. 30), but it is also related to the essentially relativistic origin of the binding energy  $\varepsilon = m_\alpha + m_\beta - M_{\{\alpha\beta\}} \neq 0$ .

At present there is no unambiguous method of including relativistic effects in calculations of processes involving bound hadronic systems. Different approaches give different results which agree only in the nonrelativistic limit. The widely used (see Ref. 31 and references therein) relativistic approach based on going to the infinite-momentum frame—noncovariant light-cone dynamics—at intermediate energies leads to explicit violation of rotational invariance, and so we do not use it here. A more systematic approach is covariant light-cone dynamics, which has been developed successfully<sup>32</sup> for problems involving the electromagnetic interaction of particles with the deuteron. This approach has not been used in practice to describe hadron–deuteron interaction processes. Recently, considerable progress has been made in developing methods for numerically solving the Bethe–Salpeter equation in Minkowski space for one-boson exchange  $NN$  potentials in the ladder approximation.<sup>33–35</sup> However, the systematic use of the Bethe–Salpeter equation is possible only in the relativistic two-body problem, and not in three-body problems such as the inclusion of three-particle  $N-\Delta-N$  forces in the  $pd$  interaction. Therefore, to include relativistic effects here we use the relativistic quantum mechanics (RQM) of systems with a fixed number of particles,<sup>36</sup> formulated on the basis of construction of the complete set of Poincaré generators.

It is often assumed that the inclusion of relativistic effects necessarily leads to quantum field theory, i.e., the inclusion of an infinite number of degrees of freedom, and so it is not possible to separate the contribution of relativistic effects from that of meson and quark degrees of freedom. However, there are arguments that, at least in the  $(v/c)^2$  approximation, a model with a fixed number of particles is a good approximation to few-nucleon systems.<sup>37</sup> An example is quantum electrodynamics, which is a potential theory in the  $(v/c)^2$  approximation (Ref. 37). Moreover, convincing evidence for the approximation of a fixed number of particles is the fact that the phase shifts of  $NN$  scattering are elastic in the lowest partial waves up to energies 1–1.5 GeV, i.e., considerably higher than the  $\pi$ -meson production threshold. In RQM the equation for the eigenvalues and eigenfunctions of the mass operator of a system of two bodies with equal masses has the same form as the Schrödinger equation.<sup>38</sup> Therefore, despite the constraint of a fixed number of particles, which is an approximation, in this approach it becomes possible to make use of the rich phenomenological

information on the  $NN$  potential obtained within the Schrödinger formulation in a completely self-consistent manner.

From the formal mathematical point of view, the main problems with the relativistic description of composite (interacting) systems arise from the more complicated structure of the generators of the Poincaré group compared to the Galilean group. The problem of incorporating the interaction is central to the RQM approach and is closely related to the problem of separating the internal and global motion. In RQM it has been shown that when the interaction is included only in the mass operator, the internal motion can be separated from the center-of-mass motion without violating the commutation relations between the generators of the Poincaré group, i.e., while preserving the relativistic invariance. The mass operator for a three-body system was first constructed in RQM in Ref. 36 on the basis of light-cone dynamics, and later in other forms of dynamics<sup>39</sup> using the method of Sokolov packing operators.<sup>40</sup> This result has been used to construct the scattering theory and to prove the relativistic invariance of the  $S$  matrix, which allows calculations to be performed in any reference frame. It is simplest to study the scattering problem in the c.m. frame, where it is sufficient to follow only the internal motion.

Of the many (unitarily equivalent<sup>41</sup>) forms of relativistic dynamics, i.e., methods of splitting the 10 Poincaré generators into Hamiltonian and kinematical operators,<sup>42</sup> the most natural from the viewpoint of the experience gained from the nonrelativistic description is the instantaneous form of the dynamics. Each form of the dynamics corresponds to a particular hypersurface in Minkowski space on which the state vector is specified and which is invariant under the action of the kinematical generators, but noninvariant under the action of the Hamiltonian ones. In instantaneous dynamics the state is specified on the hypersurface  $t = \text{const}$  in Minkowski space, and the kinematical generators are the generators of spatial translations  $\mathbf{P}$  and rotations  $\mathbf{J}$ , while the generators of Lorentz boosts  $\mathbf{N}$  and time translations  $\hat{H}$  contain the interaction. The wave function of the bound state of two particles  $\{\alpha\beta\}$  is the projection of the state vector of this system on states of the free particles  $\alpha$  and  $\beta$  with on-shell 3-momenta  $\mathbf{p}_\alpha$  and  $\mathbf{p}_\beta$ , i.e.,  $p_\alpha^2 = m_\alpha^2$  and  $p_\beta^2 = m_\beta^2$ , and  $P_{\{\alpha\beta\}}^2 = M_{\{\alpha\beta\}}^2$ , where  $m_i$  is the mass of the  $i$ th particle and  $p_i$  is its 4-momentum. The wave function of a moving two-particle bound system with total momentum  $\mathbf{P}_{\alpha\beta}$  in instantaneous dynamics has the form

$$\langle \mathbf{p}_\alpha \mathbf{p}_\beta | \mathbf{P}_{\{\alpha\beta\}} \Psi_{\{\alpha\beta\}} \rangle = (2\pi)^3 2 \sqrt{E_{\{\alpha\beta\}}(E_\alpha + E_\beta)} \delta^{(3)} \times (\mathbf{p}_\alpha + \mathbf{p}_\beta - \mathbf{P}_{\alpha\beta}) \Psi_{\{\alpha\beta\}}(\mathbf{q}_{\alpha\beta}). \quad (1)$$

Here  $E_\alpha = \sqrt{\mathbf{p}_\alpha^2 + m_\alpha^2}$ ,  $E_\beta = \sqrt{\mathbf{p}_\beta^2 + m_\beta^2}$ , and  $E_{\{\alpha\beta\}} = \sqrt{\mathbf{P}_{\{\alpha\beta\}}^2 + M_{\{\alpha\beta\}}^2}$ . This wave function is an eigenfunction of the operators for the total 4-momentum ( $\hat{P} = \hat{E}, \hat{\mathbf{P}}$ ), the squared total angular momentum  $\hat{\mathbf{J}}^2$ , and its projection  $\hat{J}_z$ . The internal wave function  $\Psi_{\{\alpha\beta\}}(\mathbf{q}_{\alpha\beta})$  in (1) is an eigenfunction of the squared mass operator  $\hat{M}^2$ , the squared angular momentum, and its projection. The separation of the variables describing the c.m. motion  $\mathbf{P}_{\alpha\beta}$  and the internal

motion  $\mathbf{q}_{\alpha\beta}$  in (1) follows immediately from the structure of the generators of the Poincaré group, where the relative momentum  $\mathbf{q}_{\alpha\beta}$  has the form

$$\mathbf{q}_{\alpha\beta} = \frac{(\varepsilon_\beta + E_\beta) \mathbf{p}_\alpha - (\varepsilon_\alpha + E_\alpha) \mathbf{p}_\beta}{\varepsilon_\alpha + E_\alpha + \varepsilon_\beta + E_\beta}, \quad (2)$$

with  $\varepsilon_\alpha = \sqrt{\mathbf{q}_{\alpha\beta}^2 + m_\alpha^2}$  and  $\varepsilon_\beta = \sqrt{\mathbf{q}_{\alpha\beta}^2 + m_\beta^2}$ . The corresponding variables in the point and light-cone forms of the dynamics also separate. However, it is important to bear in mind the fact that the variable separation is not covariant. According to Ref. 36, in calculating the transition matrix elements for the collision of a free particle  $\gamma$  with a bound state  $\{\alpha\beta\}$ , the internal wave function of the bound state can be represented as (1) with the argument (2) only in the  $\gamma + \{\alpha\beta\}$  c.m. frame (the corresponding transition operators have also been constructed<sup>36</sup> in this inertial reference frame). In going to any other inertial frame, the equation of the hypersurface ( $t = \text{const}$ ) on which the state is specified changes form, and so the form of the dynamics in which the same physical state is described also changes. In particular, in going to a different reference frame, the 3-momentum conservation at the vertex  $\{\alpha\beta\} \rightarrow \alpha + \beta$  expressed by the  $\delta$  function in (1) is violated.

In the covariant approach of Karmanov,<sup>32</sup> the wave function of the system is constructed such that the form of the dynamics appears explicitly [here we mean the various orientations of the plane  $\omega x = \omega_0 ct - \omega \mathbf{x} = 0$ , where  $\omega^2 = 0$  and  $\omega = (\omega_0, \boldsymbol{\omega})$ ]:  $\Psi(\mathbf{n}, \mathbf{q})$ , where the unit vector  $\mathbf{n} = \boldsymbol{\omega}/|\boldsymbol{\omega}|$  indexes the form of the dynamics. The dependence on  $\mathbf{n}$  is dynamical, i.e., it is determined by the form of the interaction and can be found only by solving the corresponding dynamical equations. The presence of an additional vector argument in the wave function increases the number of its components: instead of the two components in the nonrelativistic case, in the covariant approach<sup>32</sup> there are 6 components, while in the Bethe–Salpeter formalism there are 8. From the viewpoint of the Bethe–Salpeter formalism, the extra components are associated with the contribution of  $N\bar{N}$  states in the deuteron. The covariant approach is more attractive aesthetically, but when it is actually used the nontrivial problem arises of eliminating the unphysical dependence of the observables on the vector  $\mathbf{n}$ , which is in fact a consequence of the approximate nature of the calculations. This dependence must vanish in a natural way in the complete calculation. At present, this problem has been solved successfully only for elastic  $ed$  scattering<sup>43</sup> and near-threshold deuteron disintegration<sup>44</sup>  $d(e, e')pn$ .

The covariant and noncovariant approaches can be compared for the example of calculating the electromagnetic form factor of the deuteron. The free-current approximation is usually used in calculations of the electromagnetic form factor of a bound system. In this approximation the electromagnetic current operator of the bound system, being a 4-vector, does not have the correct transformation properties under the operators of the Poincaré group. Both in the covariant approach<sup>32</sup> and in the noncovariant approach the result is certainly approximate. For example, the covariant approach in the impulse approximation gives 8 extra (unphysi-

cal) form factors coupled to the additional tensor structure of the transition amplitude due to the 4-vector  $\omega$ . The covariant formulation allows the interesting possibility of going beyond the impulse approximation without any additional calculations. In particular, the physical requirement of the independence of observables from the orientation of the hypersurface of the states (i.e., the vector  $\omega$ ), can be used to discard the unphysical form factors by hand and thereby effectively include graphs more complicated than the triangle graph.<sup>1)</sup> In the noncovariant approach the result obtained in the impulse approximation for the current (usually light-cone dynamics with current component  $J^+$ ) explicitly does not satisfy rotational invariance, and from the viewpoint of the covariant approach it contains the contribution of unphysical form factors. However, it should be stressed that if a method is found for constructing the correct electromagnetic current operator of an interacting system (one version of the solution gives the impulse approximation in point dynamics<sup>45</sup>), then to obtain the exact (i.e., relativistically invariant) result in the noncovariant approach for physical observables within the approximation of a fixed number of particles, it is sufficient in principle to choose only a single particular form of the dynamics and a single inertial reference frame.

To conclude this brief aside about the problem of relativistic composite systems, we stress that all the relativistic approaches, except for RQM (Refs. 36–38, and 45), deal only with a two-particle relativistic bound state, whereas in the case of  $pd$  collisions it is actually necessary to solve the relativistic three-body problem. This is one of the main arguments in favor of using the RQM approach. Moreover, approaches which include the contribution of  $N\bar{N}$  components in the deuteron wave function are not yet developed enough to describe the experimental data on the  $NN$  phase shifts, i.e., to make the properties of the bound state consistent with those of the scattering states. In some studies (see, for example, Ref. 46), the extra components are written down purely phenomenologically from considerations of relativistic covariance without discussing the problem of constructing the relativistic  $NN$  potential and solving the corresponding equations for the wave function. Meanwhile, in RQM the properties of the bound states are consistent with those of the scattering states at the dynamical level.

### 3. THE SPIN STRUCTURE OF THE AMPLITUDE FOR THE PROCESS $\frac{1}{2} + 1 \rightarrow \frac{1}{2} + 1$

Here we give the formalism based on expansion of the reaction matrix element in invariant amplitudes. Owing to its universality, this formalism is a very efficient method of calculating both the spin-averaged differential cross sections and the polarization characteristics.

The matrix element of the process  $\frac{1}{2} + 1 \rightarrow \frac{1}{2} + 1$  can be written as

$$\langle N' \mu', \lambda' d' | T | N \mu, \lambda d \rangle = \varphi_{\mu'}^+ e_{\beta}^{(\lambda')} * e_{\alpha}^{(\lambda)} T_{\beta\alpha}(\mathbf{k}, \mathbf{k}', \sigma) \varphi_{\mu}, \quad (3)$$

where  $\varphi_{\mu}$  ( $\varphi_{\mu'}$ ) is the Pauli spinor of the initial (final) proton in the state with spin projection  $\mu$  ( $\mu'$ ),  $e_{\alpha}^{(\lambda)}$  ( $e_{\beta}^{(\lambda')}$ ) is the polarization vector of the initial  $d$  (final  $d'$ ) deuteron in the

state with spin projection  $\lambda$  ( $\lambda'$ ), and  $\beta, \alpha = x, y, z$ . Owing to rotational invariance, the operator  $T_{\beta\alpha} = T_{\beta\alpha}(\mathbf{k}, \mathbf{k}', \sigma)$  is a rank-2 tensor. This operator can be written as the tensor product of two vectors  $T_{\beta}(\mathbf{k}, \mathbf{k}', \sigma)$  and  $T_{\alpha}(\mathbf{k}, \mathbf{k}', \sigma)$ , each of which in turn can be written as an expansion:

$$\mathbf{T} = A(\mathbf{k}, \mathbf{k}', \sigma) \mathbf{n} + B(\mathbf{k}, \mathbf{k}', \sigma) \mathbf{l} + C(\mathbf{k}, \mathbf{k}', \sigma) \mathbf{m}. \quad (4)$$

Here  $\mathbf{k}(\mathbf{k}')$  is the relative momentum in the initial (final) state of the process,  $\sigma$  are the Pauli matrices, and

$$\mathbf{n} = [\mathbf{k} \times \mathbf{k}'] / |\mathbf{k} \times \mathbf{k}'|, \quad \mathbf{m} = (\mathbf{k} - \mathbf{k}') / |\mathbf{k} - \mathbf{k}'|,$$

$$\mathbf{l} = (\mathbf{k} + \mathbf{k}') / |\mathbf{k} + \mathbf{k}'|.$$

As a result, we have

$$\begin{aligned} T_{\alpha\beta}(\mathbf{k}, \mathbf{k}', \sigma) = & A_{11} n_{\alpha} n_{\beta} + A_{12} n_{\alpha} l_{\beta} + A_{13} n_{\alpha} m_{\beta} + A_{21} l_{\alpha} n_{\beta} \\ & + A_{22} l_{\alpha} l_{\beta} + A_{23} l_{\alpha} m_{\beta} + A_{31} m_{\alpha} n_{\beta} \\ & + A_{32} m_{\alpha} l_{\beta} + A_{33} m_{\alpha} m_{\beta}, \end{aligned} \quad (5)$$

where  $A_{ij}$  are scalars in  $R_3$ :

$$A_{ij} = a_{ij} + b_{ij} \mathbf{n} \sigma + c_{ij} \mathbf{l} \sigma + d_{ij} \mathbf{m} \sigma, \quad (6)$$

and  $a_{ij}$ ,  $b_{ij}$ ,  $c_{ij}$ , and  $d_{ij}$  are scalar functions of  $\mathbf{k}$  and  $\mathbf{k}'$ . The 36 complex numbers in (5) correspond to the  $2 \times 3 \times 2 \times 3 = 36$  spin amplitudes of this process. The  $P$  invariance of the matrix element (3) reduces to invariance of the tensor contraction  $e_{\beta}^{(\lambda)} e_{\alpha}^{(\lambda')} T_{\beta\alpha}$  under the operation  $\mathbf{r} \rightarrow -\mathbf{r}$ , which leads to the relation

$$T_{\alpha\beta}(-\mathbf{k}, -\mathbf{k}', \sigma) = T_{\alpha\beta}(\mathbf{k}, \mathbf{k}', \sigma). \quad (7)$$

Taking into account the properties of the vectors  $\mathbf{k}$ ,  $\mathbf{k}'$ , and  $\sigma$  under coordinate inversion, from (5)–(7) we find

$$\begin{aligned} T_{\alpha\beta}(\mathbf{k}, \mathbf{k}', \sigma) = & (a_{11} + b_{11} \mathbf{n} \sigma) n_{\alpha} n_{\beta} + (c_{12} \mathbf{l} \sigma \\ & + d_{12} \mathbf{m} \sigma) n_{\alpha} l_{\beta} + (c_{13} \mathbf{l} \sigma + d_{13} \mathbf{m} \sigma) n_{\alpha} m_{\beta} \\ & + (c_{21} \mathbf{l} \sigma + d_{21} \mathbf{m} \sigma) l_{\alpha} n_{\beta} + (a_{22} \\ & + b_{22} \mathbf{n} \sigma) l_{\alpha} l_{\beta} + (a_{23} \\ & + b_{23} \mathbf{n} \sigma) l_{\alpha} m_{\beta} + (c_{31} \mathbf{l} \sigma + d_{31} \mathbf{m} \sigma) m_{\alpha} n_{\beta} \\ & + (a_{32} + b_{32} \mathbf{n} \sigma) m_{\alpha} l_{\beta} + (a_{33} \\ & + b_{33} \mathbf{n} \sigma) m_{\alpha} m_{\beta}. \end{aligned} \quad (8)$$

In the case of elastic scattering ( $d = d'$ ,  $N = N'$ ),  $T$  invariance imposes additional constraints on the number of independent invariant amplitudes. The expressions for this case have been obtained in Ref. 8. We shall give these expressions here for completeness. Under time reversal  $t \rightarrow -t$  we have

$$\mathbf{k} \rightarrow -\mathbf{k}', \quad \mathbf{k}' \rightarrow -\mathbf{k}, \quad \mathbf{n} \rightarrow -\mathbf{n}, \quad \mathbf{l} \rightarrow -\mathbf{l}, \quad \mathbf{m} \rightarrow \mathbf{m}, \quad \sigma \rightarrow -\sigma,$$

where the initial and final states change places. Therefore, the invariance of the elastic scattering amplitude under time reversal reduces to the expression

$$T_{\beta\alpha}(\mathbf{k}, \mathbf{k}', \sigma) = T_{\alpha\beta}(-\mathbf{k}', -\mathbf{k}, -\sigma). \quad (9)$$

It follows from (9) that additional constraints are imposed on the expansion coefficients in (8):



$$\begin{aligned} c_{12} &= c_{21}, & d_{12} &= -d_{21}, & c_{13} &= -c_{31}, \\ d_{13} &= d_{31}, & a_{23} &= -a_{32}, & b_{32} &= -b_{23}. \end{aligned} \quad (10)$$

Therefore, the six additional relations (10) in the case of elastic scattering of the type  $\frac{1}{2} + 1 \rightarrow \frac{1}{2} + 1$  imply that of the 18 amplitudes in (8), only the 12 invariant amplitudes are independent. Let us choose the coordinate system such that  $OZ \uparrow \uparrow \mathbf{l}$ ,  $OY \uparrow \uparrow \mathbf{n}$ , and  $OX \uparrow \uparrow \mathbf{m}$ . Here  $n_y = l_z = m_x = 1$  (the other components of the axes are zero), and then from (8) using (10) we find

$$\begin{aligned} T_{xx} &= M_1 + M_2 \sigma_y, & T_{xy} &= M_7 \sigma_z + M_8 \sigma_x, \\ T_{xz} &= M_9 + M_{10} \sigma_y, \\ T_{yx} &= -M_7 \sigma_z + M_8 \sigma_x, & T_{yy} &= M_3 + M_4 \sigma_y, \\ T_{yz} &= M_{11} \sigma_x + M_{12} \sigma_z, \\ T_{zx} &= -M_9 - M_{10} \sigma_y, & T_{zy} &= -M_{11} \sigma_x + M_{12} \sigma_z, \\ T_{zz} &= M_5 + M_6 \sigma_y. \end{aligned} \quad (11)$$

All observables can easily be expressed in terms of the invariant amplitudes  $M_1, \dots, M_{12}$ . The cross section for the process with unpolarized particles has the form

$$\frac{d\sigma}{d\Omega} = \frac{1}{64\pi^2 s} \frac{1}{3} B, \quad (12)$$

where  $s = (p_p + p_d)^2$  and

$$B = \sum_{i=1}^{i=6} |M_i|^2 + 2 \sum_{i=7}^{i=12} |M_i|^2. \quad (13)$$

The polarization of the secondary proton  $\langle \sigma_i \rangle$  and the tensor and vector polarizations of the final deuteron  $P_i$  and  $P_{ij}$  are given by

$$\langle \sigma_i \rangle = \frac{1}{2} Sp(\rho^p \sigma_i), \quad P_i = Sp(\rho^d S_i), \quad P_{ij} = Sp(\rho^d S_{ij}), \quad (14)$$

where  $\rho^p$  and  $\rho^d$  are the polarization density matrices of the final proton and deuteron,  $S$  is the deuteron spin vector, and  $S_{ij} = (S_i S_j + S_j S_i) - \frac{4}{3} \delta_{ij}$ . In the case of unpolarized initial particles, the quantities  $\langle \sigma \rangle$ ,  $P_i$ , and  $P_{ij}$  can be expressed in terms of the invariant amplitudes of the process  $pd \rightarrow dp$  as

$$\begin{aligned} \langle \sigma_x \rangle &= \langle \sigma_y \rangle = 0, \\ \langle \sigma_y \rangle &= B^{-1} 2 \operatorname{Re}(M_1^* M_2 + M_3^* M_4 + M_5^* M_6 + 2M_9^* M_{10}), \\ P_x &= P_z = P_{xy} = P_{yz} = 0, \\ P_y &= 2B^{-1} \operatorname{Im}[M_9^*(M_1 + M_5) + M_{10}^*(M_2 + M_6) \\ &\quad + M_7 M_{12} + M_{11}^* M_8], \\ P_{xx} &= 1 - 3B^{-1}(|M_1|^2 + |M_2|^2 + |M_7|^2 + |M_8|^2 + |M_9|^2 \\ &\quad + |M_{10}|^2), \\ P_{zz} &= \sqrt{2} t_{20} = 1 - 3B^{-1}(|M_5|^2 + |M_6|^2 + |M_9|^2 + |M_{10}|^2 \\ &\quad + |M_{11}|^2 + |M_{12}|^2), \\ P_{yy} &= -P_{xx} - P_{zz}, \end{aligned}$$

$$\begin{aligned} P_{xz} &= -3B^{-1} \operatorname{Re}[M_9^*(M_1 - M_5) + M_{10}^*(M_2 - M_6) \\ &\quad + M_{11}^* M_8 - M_7^* M_{12}]. \end{aligned} \quad (15)$$

Expressions for the complete set of independent spin observables in the case of polarized initial and final particles in a process of the type  $\frac{1}{2} + 1 \rightarrow \frac{1}{2} + 1$  restricted to collinear kinematics have been obtained in Refs. 22 and 47. The polarization observables in the collinear kinematics of the process  $d + p \rightarrow p + d$  have also been studied in Ref. 14. Numerical calculations of the transfer coefficients of the vector and tensor polarization based on the mechanism of relativistic one-nucleon exchange for the process  $d + p \rightarrow p + d$  were performed in Ref. 48. A phenomenological spin structure of the amplitude different from that of Ref. 8 was used in Refs. 14, 22, and 47. Let us compare the phenomenology of (11) in the case of collinear kinematics with the corresponding expressions from Ref. 14. In the latter study the following  $P$ - and  $T$ -invariant expression was used for the  $pd \rightarrow dp$  amplitude with  $\mathbf{K} \parallel OZ$  and  $\mathbf{k}' \parallel OZ$ :

$$\begin{aligned} e_\beta^*(2) F_{\alpha\beta} e_\alpha(1) &= g_1 [\mathbf{e}_1 \mathbf{e}_2^* - (\mathbf{m} \mathbf{e}_1)(\mathbf{m} \mathbf{e}_2^*)] + g_2 (\mathbf{m} \mathbf{e}_1 \\ &\quad \times (\mathbf{m} \mathbf{e}_2^*)] + i g_3 \{ \boldsymbol{\sigma} [\mathbf{e}_1 \times \mathbf{e}_2^*] - (\boldsymbol{\sigma} \mathbf{m}) \\ &\quad \times (\mathbf{m} \cdot [\mathbf{e}_1 \times \mathbf{e}_2^*]) \} + i g_4 (\boldsymbol{\sigma} \mathbf{m})(\mathbf{m} \cdot [\mathbf{e}_1 \\ &\quad \times \mathbf{e}_2^*]), \end{aligned} \quad (16)$$

where  $g_1 - g_4$  are scalar functions. The last 8 terms in (16) associated with the vectors  $\mathbf{l}$  and  $\mathbf{n}$  are absent in the case of collinear kinematics ( $\mathbf{l} = \mathbf{n} = 0$ ). From (16) we easily find

$$\begin{aligned} F_{\alpha\beta} &= g_1 \delta_{\alpha\beta} + (g_2 - g_1) m_\alpha m_\beta + i g_3 \sigma_i \epsilon_{\alpha\beta i} + i (g_4 \\ &\quad - g_3) \sigma_i m_i m_j \epsilon_{\alpha\beta j}, \end{aligned} \quad (17)$$

where  $\epsilon_{\alpha\beta j}$  is the completely antisymmetric tensor,  $\epsilon_{123} = 1$ . Comparing (17) and (11), we obtain

$$\begin{aligned} M_1 &= M_3 = g_1, & M_7 &= i g_4, \\ M_{10} &= -i g_3, & M_{11} &= i g_3, & M_5 &= g_2. \end{aligned} \quad (18)$$

Direct calculations using the neutron exchange mechanism confirm the validity of (18).

#### 4. ANALYSIS OF THE REACTION $pp \rightarrow pn\pi^+$ AT 800 MEV

##### 4.1. The $\Delta$ -resonance region of the process $pd \rightarrow dp$

Backward elastic  $pd$  scattering in the energy range 0.4–0.8 GeV has a clearly expressed structure.<sup>49</sup> This structure, observed near the  $\Delta$ -isobar production threshold, has been studied<sup>2,3,50</sup> on the basis of the triangle mechanism with the virtual subprocess  $p + d \rightarrow d + \pi^+$  (Fig. 1a), the cross section for which has a resonance maximum at  $\sim 0.6$  GeV. In spite of the good description of the angular and energy dependence of the cross section, the triangle mechanism is essentially a phenomenological approach to  $T$  violation. A more systematic theoretical scheme in which the  $pd \rightarrow dp$  amplitude is expressed directly in terms of the elementary  $N + N \rightarrow N + \Delta$  amplitudes has been developed.<sup>8,51,52</sup> It was shown that an important role is played by the interference between the  $\Delta$ -resonance mechanism ( $\Delta$ ), corresponding to

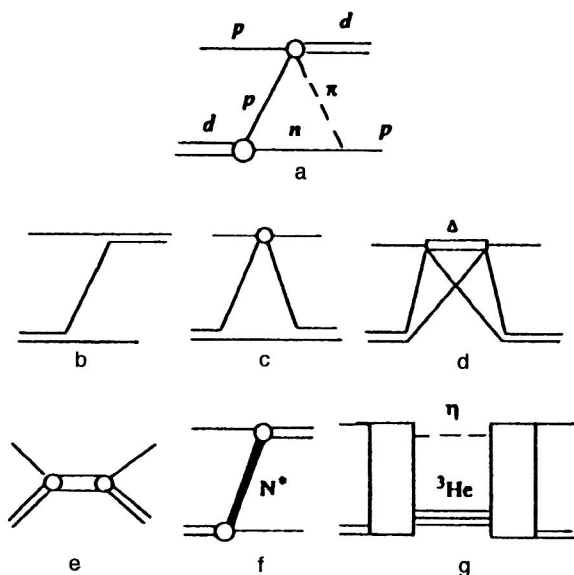


FIG. 1. Mechanisms of backward elastic  $pd$  scattering: (a) triangle graph of OPE, (b) one-nucleon exchange (ONE), (c) single  $pN$  scattering (SS), (d) the  $\Delta$  mechanism, (e) the three-baryon resonance (TBR) mechanism, (f)  $N^*$ -isobar exchange, (g) coupling of the process  $pd \rightarrow dp$  to the channel  $pd \rightarrow {}^3\text{He}\eta$ .

Fig. 1d, and the neutron-exchange mechanism (NE) (Fig. 1b), which, according to the results of Ref. 8, strongly deforms the quasiresonance maximum. Using the triangle mechanism, it is impossible to include the interference with the neutron-exchange mechanism, because the relative phase shift of the process  $pp \rightarrow d\pi^+$  is not known. The main conclusion of those studies<sup>8,51,52</sup> was that the sum of three mechanisms—the  $\Delta$ -resonance mechanism, NE in relativistic dynamics, and single  $pN$  scattering (SS) (Fig. 1c) taking into account the deuteron  $S$  and  $D$  waves—does not reproduce the characteristic shoulder in backward  $pd$  scattering in the range 0.4–0.6 GeV. The complete set of data was successfully described by introducing the contribution of three-baryon resonances (Fig. 1d). Several such resonances with mass 3.0–3.4 GeV, which in  $pd$  scattering corresponds to incident proton energy in the lab frame  $T_p \sim 0.3$ –1.0 GeV, were predicted by the model of elongated rotating bags with hidden color.<sup>53</sup> Another possible reason for this disagreement might be the contribution of nucleon-isobar exchange (Fig. 1e), the maximum contribution of which in the  $P$  wave is predicted to be at  $\sim 0.5$  GeV. Finally, there is yet another possible source of disagreement: the quasibound state in the  $\eta$ – ${}^3\text{He}$  system, indications of whose existence were found in Refs. 54 and 55 in analyzing the reaction  $pd \rightarrow {}^3\text{He}\eta$ . This state can contribute to backward elastic  $pd$  scattering at energies  $T_p \sim 1$  GeV (Fig. 1f). Therefore, the question of the mechanism of backward  $pd$  scattering in the vicinity of the  $\Delta$  resonance is of particular interest.

However, the reliability of conclusions about the contribution of exotic mechanisms is completely determined by how accurately the contribution of other, more obvious, mechanisms, primarily, double  $pN$  scattering with  $\Delta$ -isobar excitation, is calculated. According to the results of Refs. 8 and 56, this mechanism is relatively unimportant. However, in

Ref. 12 it was found that the  $\Delta$  mechanism dominates and, in conjunction with one-nucleon exchange, satisfactorily describes the data on the process  $pd \rightarrow dp$ . One reason for the disagreement between the results of Refs. 8 and 12 might be the difference in the parametrizations of the  $NN \rightarrow N\Delta$  amplitude.

The question of the parameters of the  $NN \rightarrow N\Delta$  amplitude, which is complicated in itself, becomes especially acute in this case, because the fourth power of this amplitude enters into the  $pd \rightarrow dp$  cross section. In both of the approaches under discussion, nonrelativistic parametrizations were used for the  $NN \rightarrow N\Delta$  amplitudes, and so the result of the calculation may change in going from one reference frame to another. However, the authors of those studies<sup>8,12</sup> did not verify the phenomenological expressions using other data containing information about the  $NN \rightarrow N\Delta$  amplitude in exactly the same region of kinematical variables as in the process  $pd \rightarrow dp$ . This problem has been studied<sup>57</sup> by analyzing the reaction  $pp \rightarrow pn\pi^+$ . As a result, it was concluded<sup>57</sup> that both parametrizations need to be improved, and a better parametrization of the  $NN \rightarrow N\Delta$  amplitude was found.

A theory of coupled  $NN \rightarrow \pi NN$  channels has been developed<sup>58–61</sup> for the combined description of the processes  $\pi d \rightarrow NN$ ,  $\pi d \rightarrow \pi d$ ,  $\pi d \rightarrow \pi NN$ ,  $NN \rightarrow \pi NN$ , and  $NN \rightarrow NN$  in a wide range of energies including the  $\Delta$  resonance. The  $NN \leftrightarrow N\Delta$  amplitude calculated in this theory by solving the corresponding system of coupled-channel equations will provide the most accurate answer to this interesting question. The greatest progress in this area was made in Refs. 58–60, where the Hamiltonian of the unitary approach was used to simultaneously describe the  $NN \rightarrow NN$  and  $NN \rightarrow \pi NN$  processes with a single free parameter (the mass cutoff in the meson–baryon form factors  $\Lambda_\pi = \Lambda_\rho$ ), which was found to be 0.65 GeV. Nevertheless, the agreement between the theory and the experimental data on the reaction  $pp \rightarrow pn\pi$  at  $T = 0.8$  GeV in Ref. 60 is only qualitative. In particular, the polarization characteristics are not reproduced. Therefore, to describe the  $pd \rightarrow dp$  reaction it appears justified to use the simple phenomenological  $NN \rightarrow N\Delta$  amplitude with the spin structure of one-meson  $\pi$  and  $\rho$  exchange, instead of the approach of Refs. 58–60. The parameters of this amplitude can be fixed using the kinematically complete data on the  $pp \rightarrow pn\pi^+$  reaction at 0.8 GeV (Refs. 62 and 63). This reaction is suitable because in the model of one-meson  $\pi$  and  $\rho$  exchange for the  $pp \rightarrow pn\pi^+$  amplitude, the values of the squared 4-momenta of the virtual mesons and the  $\Delta$  isobar are very close to the corresponding values of the  $\Delta$ -resonance amplitude of the process  $pd \rightarrow dp$ . Moreover, the earlier analysis of this reaction using a more fundamental approach<sup>60</sup> allows the accuracy of the approximation to be controlled.

In calculating the  $\Delta$ -resonance amplitude of the reaction  $pd \rightarrow dp$ , the amplitude of the process  $NN \leftrightarrow N\Delta$  is taken outside the integral over the relative momentum of the nucleons in the deuteron  $q_{pn}$  at the point  $q_{pn} = 0$  (Ref. 56). Therefore, the  $NN \leftrightarrow N\Delta$  amplitude enters into the final result for small momenta of the nucleons in the deuteron  $[(p_N^2 - m_N^2)/2m_N \sim -\varepsilon]$ , where  $\varepsilon$  is the deuteron binding

energy and  $p_N$  and  $m_N$  are the nucleon 4-momentum and mass]. The invariant mass of the  $\Delta$  isobar  $\mu_\Delta$  lies in the range  $\mu_\Delta = 1.15 - 1.25$  GeV for incident proton energies in the range  $T_p = 0.5 - 0.8$  GeV. It is important to note that in this approximation (i.e., when the  $NN \leftrightarrow N\Delta$  amplitude is taken out of the integral at the point  $q_{pn} = 0$ ), in scattering at  $\theta_{c.m.} = 180^\circ$  the  $\Delta$  isobar is at rest in the  $p + d$  c.m. frame at any initial energy. Therefore, the  $NN \rightarrow N\Delta$  amplitude in the  $\Delta$  rest frame enters into the amplitude of the process  $pd \rightarrow dp$  calculated in the c.m. frame of the proton and deuteron, and so the static approximation can be used.

The results of the analysis of the reaction  $pp \rightarrow pn\pi^+$  obtained earlier using the one-meson exchange model cannot be used directly to construct the  $NN \rightarrow N\Delta$  amplitude for the process  $pd \rightarrow dp$ . For example, straightforward calculations show that in the nonrelativistic approach<sup>62</sup> the result depends on the choice of reference frame and, despite the fact that Galilean corrections are included, the reaction cross section is not reproduced if the reaction amplitude is calculated in the  $\Delta$ -isobar rest frame. On the other hand, a Lorentz-invariant analysis<sup>64</sup> including the complete set of parameters of both the inclusive and the exclusive data at initial energies  $\sim 0.8$  GeV does not give a good description of the reaction  $pp \rightarrow pn\pi^+$ . Several years after the publication of Ref. 57, new parametrizations appeared for the  $NN \rightarrow N\Delta$  amplitude based on both the noncovariant formalism of  $\pi + \rho$  exchange<sup>65</sup> and the fully covariant model of one-boson exchange.<sup>66</sup> The parametrization obtained in Ref. 65 is very close in form to that of Ref. 57. The only difference is in the numerical values of the cutoff parameters in the form factors, which is apparently related to the presence of the additional Landau–Migdal term in the structure of the amplitude. To systematically apply the covariant formalism<sup>66</sup> to the  $pd \rightarrow dp$  process with the  $\Delta$ -resonance mechanism, it is necessary to have a fully covariant formulation of the amplitude of this mechanism, which at present is not available in the literature.

#### 4.2. The $NN \rightarrow N\Delta$ amplitude

In Ref. 57 the reaction  $pp \rightarrow pn\pi^+$  was described by including the contribution of the four graphs shown in Fig. 2, the amplitudes of which were calculated in the  $\Delta$ -isobar rest frame. The static approximation  $p_\Delta = 0$  for the Rarita–Schwinger spinor  $\Psi_\mu$  describing the  $\Delta$  isobar was used, as well as the relativistic form of the  $\pi NN$  and  $\rho NN$  vertices. The contribution of other such graphs containing  $N$  and  $N^*$  instead of the  $\Delta$  isobar is  $\leq 1\%$  in this kinematical region<sup>62</sup> and so is neglected. In this region the relative energy of the nucleons is  $\geq 15$  MeV, and so the  $np$  final-state interaction does not dominate.<sup>60</sup> As shown in Ref. 60, the interaction in the initial ( $NN$ ) and final ( $N\Delta$ ) states of the process  $NN \rightarrow N\Delta$  decreases the cross section for the reaction  $pp \rightarrow pn\pi^+$  by no more than 30% compared to one-meson  $\pi$ - and  $\rho$ -exchange in the plane-wave approximation, and does not change the shape of the distribution. The effect of the initial- and final-state interactions is obviously masked in the parameters of the form factors. Using the phenomeno-

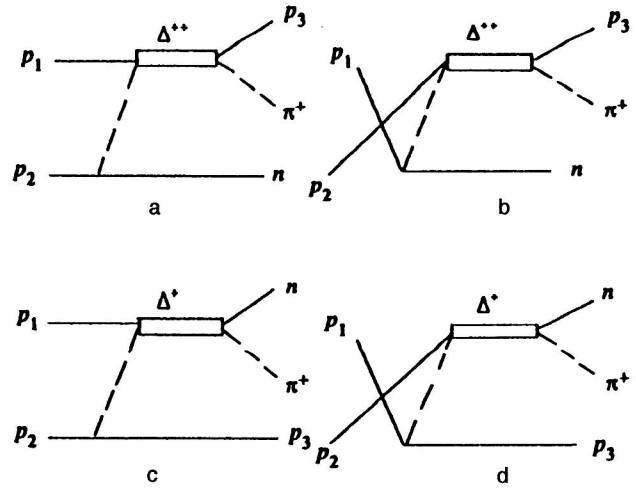


FIG. 2. Mechanism for the reaction  $pp \rightarrow pn\pi^+$  in the  $\Delta$ -resonance production region.

logical interaction Lagrangians  $L_{\pi NN}$ ,  $L_{\rho NN}$ ,  $L_{\pi N\Delta}$ , and  $L_{\rho N\Delta}$  given in Ref. 64, for the meson–baryon vertices we have

$$\langle \pi N_2 | N_1 \rangle = (f_{\pi NN} / m_\pi) \varphi_1^+ (\sigma \mathbf{Q}) (\boldsymbol{\tau} \boldsymbol{\Phi}_\pi) \varphi_2 2m_N, \quad (19)$$

$$\langle \rho N_2 | N_1 \rangle = (f_{\rho NN} / m_\rho) \varphi_1^+ ([\sigma \mathbf{Q}] \boldsymbol{\epsilon}_\rho) (\boldsymbol{\tau} \boldsymbol{\Phi}_\rho) \varphi_2 2m_N, \quad (20)$$

$$\langle \pi N | \Delta \rangle = f_{\pi N\Delta} / m_\pi (\boldsymbol{\Psi}_\Delta^+ \mathbf{Q}'_\pi) (\mathbf{T} \boldsymbol{\Phi}_\pi) \varphi \sqrt{2m_N 2m_\Delta}, \quad (21)$$

$$\langle \rho N | \Delta \rangle = (f_{\rho N\Delta} / m_\rho) ([\boldsymbol{\Psi}_\Delta^+ \mathbf{Q}'_\rho] \boldsymbol{\epsilon}_\rho) (\mathbf{T} \boldsymbol{\Phi}_\rho) \varphi \sqrt{2m_N 2m_\Delta}, \quad (22)$$

where

$$f_{\pi NN} = 1.00, \quad f_{\pi N\Delta} = 2.15, \quad f_{\rho NN} = 6.20, \quad f_{\rho N\Delta} = 13.33.$$

Here  $\varphi$  is the Pauli spinor of the nucleon,  $\boldsymbol{\Psi}_\Delta$  is the static vector spinor of the  $\Delta$  isobar,  $\boldsymbol{\Phi}_\pi$  and  $\boldsymbol{\Phi}_\rho$  are the isovector wave functions of the  $\pi$  and  $\rho$  mesons,  $\boldsymbol{\epsilon}_\rho$  is the  $\rho$ -meson polarization vector,  $\boldsymbol{\tau}$  is the Pauli isospin matrix, and the isospin operator  $\mathbf{T}$  is defined in Ref. 62.

The momentum  $\mathbf{Q}$  in (19) and (20) has the form

$$\mathbf{Q} = \left[ \frac{E_2 + m_N}{E_1 + m_N} \right]^{1/2} \mathbf{p}_1 - \left[ \frac{E_1 + m_N}{E_2 + m_N} \right]^{1/2} \mathbf{p}_2, \quad (23)$$

$E_i = \sqrt{p_i^2 + m_N^2}$  is the total nucleon energy. In Eqs. (19)–(22),  $\mathbf{Q}'_\pi$  ( $\mathbf{Q}'_\rho$ ) is the virtual  $\pi$  ( $\rho$ ) momentum in the  $\Delta$ -isobar rest frame, i.e., the relative momentum in the  $\pi(\rho) + N$  frame. On the mass shell, the relativistic relative momentum  $\mathbf{Q}'_\pi$  in the  $\pi + N$  frame has the form

$$\mathbf{Q}'_\pi = \frac{(\tilde{E} + \varepsilon_N) \tilde{\mathbf{P}}_\pi - (\tilde{E}_\pi + \varepsilon_N) \tilde{\mathbf{P}}_N}{\tilde{E}_N + \varepsilon_N + \tilde{E}_\pi + \varepsilon_\pi}, \quad (24)$$

where  $\varepsilon_i$  is the energy of the  $i$ th particle in the  $\pi + N$  c.m. frame, and  $\tilde{E}_i$  and  $\tilde{\mathbf{P}}_i$  are its energy and momentum in an arbitrary inertial frame. For the momenta of the virtual  $\pi$  and  $\rho$  mesons  $\mathbf{Q}'_\pi$  and  $\mathbf{Q}'_\rho$  we use equations analogous to (24), with the replacement  $m_\pi^2 \rightarrow q_\pi^2$  and  $m_\rho^2 \rightarrow q_\rho^2$  in the expressions for the total energy. For the  $\Delta$  propagator we use the

nonrelativistic expression with mass  $m_\Delta \rightarrow m_\Delta - i\Gamma/2$ , in which the total width  $\Gamma$  includes the off-shell nature of the  $\Delta$  isobar:

$$\Gamma(k) = \Gamma_0 \left( \frac{k}{k_R} \right)^3 \frac{k_R^2 + \chi^2}{k^2 + \chi^2}. \quad (25)$$

Here  $\Gamma_0 = 120$  MeV,  $\chi = 180$  MeV/c,  $k_R$  and  $k$  are the  $\pi$ -meson momenta at the resonance and away from it, respectively,

$$k^2 = q_\pi^2 = [\mu_\Delta^2 - (m_N - m_\pi)^2][\mu_\Delta^2 - (m_N + m_\pi)^2]/4\mu^2 m, \quad (26)$$

and  $\mu_\Delta^2$  is the squared 4-momentum of the  $\Delta$  isobar. At the vertex of off-shell decay of the  $\Delta$  isobar into a real  $\pi$  meson and nucleon we use not the constants  $f_{\pi N\Delta}/m_\pi$ , but rather the form factor

$$G(k^2) = (f_{\pi N\Delta}/m_\pi)Z(k^2), \quad (27)$$

where

$$Z(k^2) = [(k_R^2 + \chi^2)/(k^2 + \chi^2)]^{1/2}. \quad (28)$$

Equations (25) and (27) were motivated by the analysis of the  $\delta_{33}$  phase shifts of elastic  $\pi p$  scattering. At the  $\Delta$ -isobar production vertices  $\pi p \rightarrow \Delta$  and  $p p \rightarrow \Delta$ , and also at the  $\pi NN$  and  $\rho NN$  vertices, the corresponding constants are multiplied by form factors taking into account the off-shell nature of the mesons:

$$F_{\pi NN}(q^2) = F_{\pi N\Delta}(q^2) \equiv F_\pi(q^2) = (\Lambda_\pi^2 - m_\pi^2)/(\Lambda_\pi^2 - q^2),$$

$$F_{\rho NN}(q^2) = F_{\rho N\Delta}(q^2) \equiv F_\rho(q^2) = (\Lambda_\rho^2 - m_\rho^2)/(\Lambda_\rho^2 - q^2), \quad (29)$$

where  $q^2$  is the squared meson 4-momentum. The cutoff parameters  $\Lambda_\pi$  and  $\Lambda_\rho$  are determined so as to best describe the experimental data. Let us give the expression for the  $NN \rightarrow N\Delta$  amplitude, for example, entering into the graph of Fig. 2a:

$$A_a^{(\pi+\rho)}(NN \rightarrow N\Delta) = (\Psi_i^+ \varphi_1) \times (\varphi_n^+ \sigma_k \varphi_2) \mathcal{D}_{ik}(\mathbf{Q}_a, \mathbf{Q}'_{\pi a}, \mathbf{Q}'_{\rho a}) \quad (30)$$

where

$$\begin{aligned} \mathcal{D}_{ik}(\mathbf{Q}, \mathbf{Q}'_\pi, \mathbf{Q}'_\rho) = & \left[ \mathcal{Q}'_{\pi i} \mathcal{Q}_k \frac{f_{\pi NN} f_{\pi N\Delta}}{m_\pi^2} F_\pi(q^2) \frac{1}{q^2 - m_\pi^2} \right. \\ & + (\mathcal{Q}'_{\rho m} \mathcal{Q}_m \delta_{ik} - \mathcal{Q}'_{\rho k} \mathcal{Q}_i) \frac{f_{\rho NN} f_{\rho N\Delta}}{m_\rho^2} \\ & \left. \times F_\rho(q^2) \frac{1}{q^2 - m_\rho^2} \right] \sqrt{2m_\Delta (2m_N)^3}. \end{aligned} \quad (31)$$

The main difference between (30) and (31) and the analogous expressions in Refs. 8 and 12 is that different momenta  $\mathbf{Q} \neq \mathbf{Q}'$  enter into the  $\pi(\rho)NN$  and  $\pi(\rho)N\Delta$  vertices, while in Refs. 8 and 12 these momenta are the same. The other differences are related to the choice of parameters of the form factors.

### 4.3. The amplitude of the process $pp \rightarrow pn\pi^+$

Knowing the  $pn \rightarrow n\Delta^{++}$  amplitude and the  $\pi N\Delta$  vertex, we can write down the amplitude of the process  $pp \rightarrow pn\pi^+$ . The amplitude corresponding to the graph in Fig. 2a has the form

$$\begin{aligned} \langle \pi^2 n p | A_a | p_1 p_2 \rangle = & \sqrt{2} R(\mu_\Delta) k_l \left[ \varphi_p \left( \delta_{il} - \frac{1}{3} \sigma_l \sigma_i \right) \varphi_1 \right] \\ & \times (\varphi_n^+ \sigma_k \varphi_2) \mathcal{D}_{ik}(\mathbf{Q}_a, \mathbf{Q}'_{\pi a}, \mathbf{Q}'_{\rho a}), \end{aligned} \quad (32)$$

where

$$R(\mu_\Delta) = \frac{f_{\pi N\Delta}}{m_\pi} \frac{\sqrt{2m_\Delta 2m_p} \sqrt{Z(k^2)}}{\mu_\Delta - m_\Delta + i\Gamma(k)/2}. \quad (33)$$

The total amplitude of the process  $pp \rightarrow pn\pi^+$  obtained including the four graphs of Figs. 2a–2d can be written as

$$\begin{aligned} A(pp \rightarrow pn\pi^+) = & \sqrt{2} R(\mu_\Delta) k_l \left[ \varphi_p^+ \left( \delta_{il} - \frac{1}{3} \sigma_l \sigma_i \right) \varphi_1 \right] \\ & \times (\varphi_n^+ \sigma_k \varphi_2) \mathcal{D}_{ik}(\mathbf{Q}_a, \mathbf{Q}'_{\pi a}, \mathbf{Q}'_{\rho a}) \\ & - \sqrt{2} R(\mu_\Delta) k_l \left[ \varphi_p \left( \delta_{il} - \frac{1}{3} \sigma_l \sigma_i \right) \varphi_2 \right] \\ & \times (\varphi_n^+ \sigma_k \varphi_1) \mathcal{D}_{ik}(\mathbf{Q}_b, \mathbf{Q}'_{\pi b}, \mathbf{Q}'_{\rho b}) \\ & - \frac{\sqrt{2}}{3} R(\tilde{\mu}_\Delta) \tilde{k}_l \left[ \varphi_n \left( \delta_{il} - \frac{1}{3} \sigma_l \sigma_i \right) \varphi_1 \right] \\ & \times (\sigma_p^+ \sigma_k \varphi_2) \mathcal{D}_{ik}(\tilde{\mathbf{Q}}_c, \tilde{\mathbf{Q}}'_{\pi c}, \tilde{\mathbf{Q}}'_{\rho c}) \\ & + \frac{\sqrt{2}}{3} R(\tilde{\mu}_\Delta) \tilde{k}_l \left[ \varphi_n^+ \left( \delta_{il} - \frac{1}{3} \sigma_l \sigma_i \right) \varphi_2 \right] \\ & \times (\varphi_p^+ \sigma_k \varphi_1) \mathcal{D}_{ik}(\tilde{\mathbf{Q}}_d, \tilde{\mathbf{Q}}'_{\pi d}, \tilde{\mathbf{Q}}'_{\rho d}). \end{aligned} \quad (34)$$

Here  $\tilde{\mu}_\Delta$  is the squared 4-momentum of the virtual  $\Delta^+$  isobar and  $\tilde{k}$  is the corresponding relative momentum at the  $\Delta^+ \rightarrow n + \pi^+$  vertex. The tilde on the momenta  $\mathbf{Q}$  and  $\mathbf{Q}'$  refers to graphs containing the  $\Delta^+$  isobar, while momenta without the tilde pertain to the corresponding graph containing the  $\Delta^{++}$  isobar in the intermediate state. The subscripts a, b, c, and d on the 3-momenta refer to the corresponding graphs in Fig. 2, and  $\sqrt{2}$  and  $-\sqrt{2}/3$  are isotopic factors.

### 4.4. Results for the calculated cross section of the reaction $pp \rightarrow pn\pi^+$

In Fig. 3 we show the results for the cross section  $d^5/d\Omega_\pi d\Omega_p dp_p$  for the reaction  $pp \rightarrow pn\pi^+$  calculated as a function of the secondary proton momentum  $p_p$ . The upper scales show  $\mu_\Delta$ , the invariant mass of the  $\Delta^{++}$  isobar in the  $pp \rightarrow pn\pi^+$  reaction and  $pd$  scattering at  $\Theta_{c.m.} = 180^\circ$ , and  $q^2$  and  $a^2$  are the squared 4-momenta of the virtual  $\pi$  mesons in the dominant graphs for the  $pp \rightarrow pn\pi^+$  reaction and  $pd$  scattering at  $\Theta_{c.m.} = 180^\circ$ , respectively. The dependence of the squared 4-momentum of the virtual meson  $q^2$  on  $\mu_\Delta$  [ $q^2 = q^2(\mu_\Delta)$ ] in the reaction  $pp \rightarrow pn\pi^+$  (for the dominant graph) corresponds most closely to the analogous dependence  $a^2 = a^2(\mu_\Delta)$  in  $pd$  scattering at  $\Theta_{c.m.} = 180^\circ$  at the



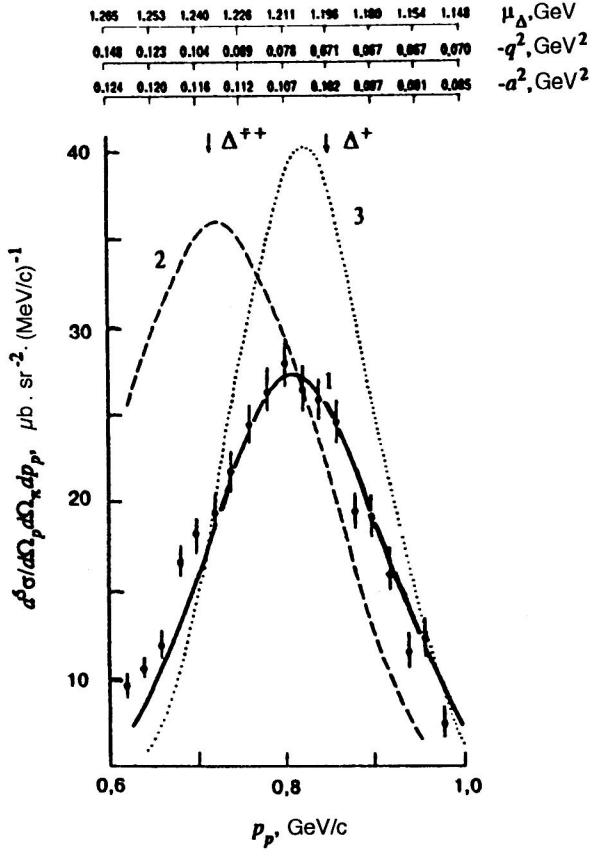


FIG. 3. Differential cross section of the reaction  $pp \rightarrow pn\pi^+$  at  $\theta_p = 15^\circ$ ,  $\theta_\pi = 20.8^\circ$  as a function of the secondary proton momentum. The curves show the calculated results: (1) calculation of Ref. 57 with  $\Lambda_\pi = 0.53$  GeV/c,  $\Lambda_\rho = 0.7$  GeV/c; (2) parametrization of Eq. (9) from Ref. 8 for  $\Lambda_\pi = 1$  GeV/c,  $\Lambda_{\rho p} = 1.167$  GeV/c,  $\Lambda_{pp} = 2.449$  GeV/c; (3) parametrization of Ref. 12 for  $\Lambda_\pi = 0.53$  GeV/c neglecting the  $\rho$ -meson contribution. The points  $\bullet$  are the experimental data from Ref. 62. See the text for explanation.

emission angles  $\Theta_p = 15^\circ$  and  $\Theta_\pi = 20.8^\circ$  taken from experiment.<sup>62</sup> This agreement worsens with increasing angle between the proton and  $\pi^+$ . The calculations show that the  $\Delta^{++}$  contribution dominates. The contribution of graphs containing the  $\Delta^+$  isobar is suppressed by both the isotopic factor of  $\frac{1}{3}$ , and the stronger off-shell nature of the virtual mesons. There is no interference between graphs a, d and b, c. However, graphs a, c and b, d do interfere owing to the intermediate states containing  $\Delta^{++}$  and  $\Delta^+$  isobars. In Fig. 3 the arrows indicate the points at which the  $\Delta^{++}$  and  $\Delta^+$  go off-shell:  $\mu_\Delta = \tilde{\mu}_\Delta = 1232$  MeV. The shift of the experimentally observed maximum to the right of the point  $\mu_{\Delta^{++}} = 1232$  MeV is due to the  $k$  dependence of the width  $\Gamma(k)$  according to (25). Assuming, in accordance with Ref. 67, that the  $\rho$ -exchange contribution is small, and taking  $\Lambda_\rho = 0.7$  GeV/c, for  $\Lambda_\pi$  we find 0.53 GeV/c, which gives the best agreement with experiment. Interestingly, this value is consistent with the prediction obtained in the Skyrme model<sup>68</sup> ( $\Lambda_\pi = 0.528$  GeV/c). The similar value  $\Lambda_\pi = 0.63$  GeV/c (for  $\Lambda_\rho = 0.7$  GeV/c) has been obtained<sup>69</sup> by analyzing the inclusive data on the reaction  $NN \rightarrow N\Delta$  at energies of a few GeV. Substituting the values  $\Lambda_\pi = \Lambda_\rho$

$= 0.65$  GeV/c, as in Ref. 60, we find that the cross section for the  $pp \rightarrow pn\pi^+$  reaction is increased by  $\sim 30\%$ .

For comparison, in Fig. 3 we give the curves obtained using the parameters for the  $NN \leftrightarrow N\Delta$  amplitudes from Refs. 8 and 12. These calculations show that both parametrizations overestimate the contribution of the  $\Delta$  isobar. Upon rescaling to the cross section for backward  $pd$  scattering, the overestimate where the  $\Delta$ -resonance mechanism contributes maximally is  $\sim 1.5$  in Ref. 8 and  $\sim 2$  in Ref. 12. The parametrization of Ref. 8 shifts the maximum of the cross section to larger  $\mu_\Delta$  by approximately 20 MeV, which is a consequence of the assumption  $\Gamma(k) = \Gamma_0$  made in Ref. 8. In addition, the approximation  $q_{pn} = 0$  mentioned above also overestimates the contribution of the  $\Delta$ -resonance mechanism to backward  $pd$  scattering. It can therefore be concluded that the pure contribution of this mechanism to the  $pd \rightarrow dp$  process is overestimated in both Ref. 8 and Ref. 12. It is natural to expect that after appropriate improvement of the parameters of the  $NN \rightarrow N\Delta$  amplitude, the contribution of other mechanisms for the process  $pd \rightarrow dp$  different from the  $\Delta$ -resonance one will be more important. However, we shall see in the following section that this guess is not confirmed owing to interference effects.

## 5. THE NE+ $\Delta$ +SS MODEL OF THE PROCESS $pd \rightarrow dp$

The NE+ $\Delta$ +SS model of the process  $pd \rightarrow dp$  was proposed in Ref. 8, and then modified with respect to the  $\Delta$ -resonance mechanism in Ref. 13. In Refs. 70 and 71 it was generalized to describe the processes  $p + (pn)_i \rightarrow d + p$  and  $p + d \rightarrow N + (NN)_{i,s}$ , where  $(NN)_{i,s}$  is the  $NN$  pair in the triplet (t) or singlet (s) state.

### 5.1. Neutron exchange

Neglecting the effect of relativistic spin rotations, as in Ref. 8, for the amplitude of the process  $pd \rightarrow dp$  in the case of the NE mechanism we have

$$T^{(NE)} = \Pi e_\gamma^{(\lambda'_d)*} e_\alpha^{\lambda_d} \phi_{\sigma'_p}^* \left\{ \sigma_\alpha u(q) - \frac{1}{\sqrt{2}} \left[ \sigma_\alpha - 3q_\alpha \frac{(\mathbf{q}\sigma)}{q^2} \right] w(q) \right\} \left\{ \sigma_\gamma u(q') - \frac{1}{\sqrt{2}} \left[ \sigma_\gamma - 3q'_\gamma \frac{(\mathbf{q}'\sigma)}{q'^2} \right] w(q') \right\} \phi_{\sigma_p}, \quad (35)$$

where  $u(q)$  and  $w(q)$  are the S and D components of the deuteron wave function in momentum space, normalized by the condition

$$\int_0^\infty [u^2(q) + w^2(q)] \frac{d^3q}{(2\pi)^3} = 1, \quad (36)$$

$\mathbf{q}$  and  $\mathbf{q}'$  are the Lorentz-invariant relative momenta at the  $\langle np \rangle \rightarrow n + p$  and  $n + p \rightarrow d$  vertices, defined according to the rules of relativistic quantum mechanics by (2),

$$\Pi = -(\sqrt{s} - E_p - E'_p - E_n) \frac{E_d E'_d}{E_n} \varepsilon(q), \quad (37)$$

$E_i = \sqrt{m_i^2 + \mathbf{p}_i^2}$  and  $\mathbf{p}_i$  are the energy and momentum of the  $i$ th particle in the  $p+d$  c.m. frame,  $\mathbf{p}_n = \mathbf{p}_d - \mathbf{p}'_d$ , and  $\varepsilon(q) = \frac{1}{2} \sqrt{(E'_p + E_n)^2 - \mathbf{p}_d^2}$ .

## 5.2. Double $pN$ scattering with $\Delta$ -isobar excitation

The amplitude of the process  $pd \rightarrow dp$  with  $\Delta$ -isobar excitation in the intermediate state can be written as the following single integral:

$$\begin{aligned} T^{(\Delta)} &= \langle \mathbf{p}'_p \phi_{\sigma'_p}, \mathbf{p}'_d \mathbf{e}_d^{(\lambda'_d)} | \tau^{(\Delta)}(pd \rightarrow pd) | \mathbf{k}_p \phi_{\sigma_p}, \mathbf{p}_d \mathbf{e}_d^{(\lambda)} \rangle \\ &= -\frac{i}{2\pi\eta(k, \Delta)} e_\gamma^{(\lambda'_d)*} e_\alpha^{\lambda_d} R_{\beta\delta} \int_0^\infty dr \\ &\quad \times \exp\left\{ \frac{2imr(m^2 + \Delta^2/4 - m_\Delta^2 + iM_\Delta\Gamma)}{\eta(k, \Delta)} \right\} \\ &\quad \times \left[ u(r) \delta_{\alpha\beta} + \frac{1}{\sqrt{2}} (\delta_{\alpha\beta} - 3n_\alpha n_\beta w(r)) \right] \\ &\quad \times \left[ u(r) \delta_{\gamma\delta} + \frac{1}{\sqrt{2}} (\delta_{\gamma\delta} - 3n'_\gamma n'_\delta w(r)) \right], \end{aligned} \quad (38)$$

where

$$\mathbf{n} = (n_x, n_y, n_z) = \left( \frac{4mk_x}{\eta(k, \Delta)}, 0, \frac{k_0\Delta}{\eta(k, \Delta)} \right),$$

$$\mathbf{n}' = (-n_x, 0, n_z),$$

$$\eta(k, \Delta) = (4k_x^2 m_d^2 + k_0^2 \Delta^2)^{1/2}, \quad \Delta = 4p_p^2 \sin^2 \frac{\theta}{2},$$

$$k_x^2 = \frac{s \mathbf{p}_p^2 \cos^2 \frac{\theta}{2}}{m_d^2 + \mathbf{p}^2 \sin^2 \frac{\theta}{2}}, \quad k_0^2 = m^2 + K_x^2 + \frac{\Delta}{4}. \quad (39)$$

Here  $u(r)$  and  $w(r)$  are the components of the deuteron wave function in coordinate space. The  $NN \leftrightarrow N\Delta$  amplitudes enter into the tensor  $R_{\beta\delta}$ . In contrast to Ref. 8, here we use the parametrization (30). The tensor  $R_{\beta\delta}$  has the form

$$\begin{aligned} R_{\beta\delta} &= \left[ \phi_{\sigma'_p}^* \sigma_m \sigma_\beta \left( \delta_{li} - \frac{1}{3} \sigma_i \sigma_l \right) \sigma_\delta \sigma_k \phi_{\sigma_p} \right] \\ &\quad \times \mathcal{D}_{ik}(\mathbf{a}, \mathbf{a}') \mathcal{D}_{lm}(\mathbf{b}, \mathbf{b}') + \left[ \phi_{\sigma'_p}^* \left( \delta_{li} \right. \right. \\ &\quad \left. \left. - \frac{1}{3} \sigma_l \sigma_i \right) \sigma_\beta \sigma_m \sigma_\delta \sigma_k \phi_{\sigma_p} \right] \mathcal{D}_{ik}(\mathbf{a}, \mathbf{a}') \mathcal{D}_{lm}(\mathbf{c}, \mathbf{c}') \\ &\quad + \left[ \phi_{\sigma'_p}^* \sigma_m \sigma_\beta \sigma_k \sigma_\delta \left( \delta_{li} - \frac{1}{3} \sigma_i \sigma_l \right) \phi_{\sigma_p} \right] \end{aligned}$$

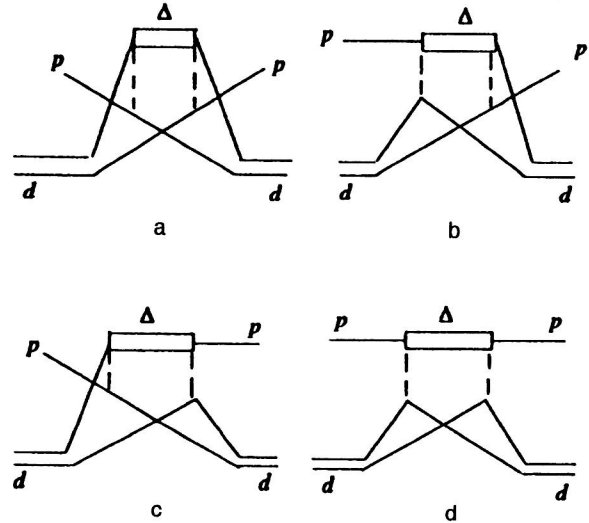


FIG. 4.  $\Delta$ -resonance mechanism for backward elastic  $pd$  scattering.

$$\begin{aligned} &\times \mathcal{D}_{ik}(\mathbf{c}, \mathbf{c}') \mathcal{D}_{lm}(\mathbf{b}, \mathbf{b}') - \left[ \phi_{\sigma'_p}^* \left( \delta_{li} \right. \right. \\ &\quad \left. \left. - \frac{1}{3} \sigma_l \sigma_i \right) S p(\sigma_k \sigma_\beta \sigma_m \sigma_\delta) \phi_{\sigma_p} \right] \\ &\quad \times \mathcal{D}_{ik}(\mathbf{c}, \mathbf{c}') \mathcal{D}_{lm}(\mathbf{c}, \mathbf{c}'). \end{aligned} \quad (40)$$

The functions  $\mathcal{D}_{ik}(\mathbf{x}, \mathbf{x}')$  and  $\mathcal{D}_{lm}(\mathbf{x}, \mathbf{x}')$  are defined as in (32). As noted in the preceding section, the vectors  $\mathbf{x}$  and  $\mathbf{x}'$  are different. In deriving (38), the  $NN \leftrightarrow N\Delta$  amplitudes were taken outside the integral over the momenta of the intermediate nucleons at the point where the relative momentum of the nucleons in the deuteron is zero. In this approximation the 4-momenta  $a'$ ,  $b'$ , and  $c'$  of the intermediate mesons are uniquely expressed in terms of the 4-momenta of the initial and final particles as

$$a' = p_p - \frac{p'_d}{2}, \quad b' = \frac{p_d}{2} - p'_p, \quad c' = \frac{p'_d - p_d}{2}. \quad (41)$$

The 3-momenta  $\mathbf{a}'$ ,  $\mathbf{b}'$ , and  $\mathbf{c}'$  corresponding to the  $\pi(\rho)NN$  vertex are defined as in (23) and have the form

$$\mathbf{a} = \sqrt{\frac{E_d + m_d}{2(E_p + m_p)}} \mathbf{p}_p - \sqrt{\frac{E_p + m_p}{2(E_d + m_d)}} \mathbf{p}'_d,$$

$$\mathbf{b} = \sqrt{\frac{E_p + m_p}{2(E_d + m_d)}} \mathbf{p}_d - \sqrt{\frac{E_d + m_d}{2(E_p + m_p)}} \mathbf{p}'_p,$$

$$\mathbf{c} = \frac{\mathbf{p}'_d - \mathbf{p}_d}{2}. \quad (42)$$

The four terms in the tensor  $R_{\beta\delta}$  correspond to the contributions of the 4 graphs shown in Fig. 4. In these graphs the  $\Delta$  isobar can occur in three charge states:  $\Delta^{++}$ ,  $\Delta^+$ , and  $\Delta^0$ . It is sufficient to perform all the calculations for  $\Delta^{++}$ , and to include the contributions of the  $\Delta^+$  and  $\Delta^0$  states by the isotopic factor of 2, i.e.,  $A^{(\Delta^{++} + \Delta^+ + \Delta^0)} = 2A^{(\Delta^{++})}$ . The most important of the graphs in Fig. 4 is graph a. The contributions of the others are considerably smaller because the

intermediate mesons are farther from the mass shell. In Ref. 8 the decrease of the  $\pi N\Delta$  vertex function as the  $\Delta$  isobar moves away from the mass shell was taken into account by an auxiliary factor of the form

$$D = \frac{m_0^4}{(s - m_\Delta^2)^2 + m_0^4}, \quad (43)$$

where  $s$  is the squared 4-momentum of the  $\Delta$  isobar and  $m_0$  is a numerical parameter. As shown in the preceding section, when off-shell effects are included in this manner, it is not possible to describe the location of the experimentally observed maximum in the  $pp \rightarrow pn\pi^+$  cross section in the  $\Delta$ -resonance region. Here we include off-shell effects in a different way, namely, by introducing the factor (28) into the  $\pi N\Delta$  vertex and taking into account the  $k$  dependence of the total  $\Delta$ -isobar width (25).

### 5.3. Single pN scattering

In the SS mechanism for proton backward scattering on the deuteron, the maximum contribution comes from the exchange process, where the incident and nuclear protons change places. According to Ref. 8, the amplitude for the SS mechanism can be written as

$$T^{(SS)} = \frac{m_d}{m} \left( \frac{3}{2} A_{NN}^{(1)}(s_1, t) - \frac{1}{2} A_{NN}^{(0)} \right) \times (s_1, t) \left( e_{\gamma}^{(\lambda'_d)*} e_{\alpha}^{(\lambda)} \phi_{\sigma_p}^* M_{\alpha\gamma}^{(SS)} \phi_{\sigma_p} \right); \quad (44)$$

here  $A_{NN}^{(0)}$  and  $A_{NN}^{(1)}$  are the  $NN$  scattering amplitudes with isospin  $T=0$  and  $T=1$ , respectively. The tensor  $M_{\alpha\gamma}^{(SS)}$  in (44) is expressed in terms of integrals of products of the deuteron wave functions  $u$  and  $w$  as

$$M_{\alpha\gamma}^{(SS)} = \sigma_\alpha \sigma_\gamma W_{SS}(\Delta) - \sigma_\alpha [\sigma_\gamma - 3(N\sigma)N_\gamma] W_{SD}(\Delta) - [\sigma_\alpha - 3(N\sigma)N_\alpha] \sigma_\gamma W_{SD}(\Delta) + (3\delta_{\alpha\gamma} - \sigma_\alpha \sigma_\gamma) W_{DD0}(\Delta) + [3\delta_{\alpha\gamma} - 2\sigma_\alpha \sigma_\gamma - 9N_\alpha N_\gamma + 3\sigma_\alpha(\sigma N)N_\gamma + 3(\sigma N)N_\alpha \sigma_\gamma] W_{DD2}(\Delta), \quad (45)$$

where

$$\Delta = \mathbf{p}_p - \mathbf{p}_p', \quad \mathbf{N} = \frac{\Delta}{\Delta}$$

$$W_{SS}(\Delta) = \int_0^\infty j_0\left(\frac{\Delta}{2}r\right) u(r)^2 r^2 dr,$$

$$W_{SD}(\Delta) = \frac{1}{\sqrt{2}} \int_0^\infty j_2\left(\frac{\Delta}{2}r\right) u(r)w(r) r^2 dr,$$

$$W_{DD0}(\Delta) = \frac{1}{2} \int_0^\infty j_0\left(\frac{\Delta}{2}r\right) w(r)^2 r^2 dr,$$

$$W_{DD2}(\Delta) = \frac{1}{2} \int_0^\infty j_2\left(\frac{\Delta}{2}r\right) w(r)^2 r^2 dr. \quad (46)$$

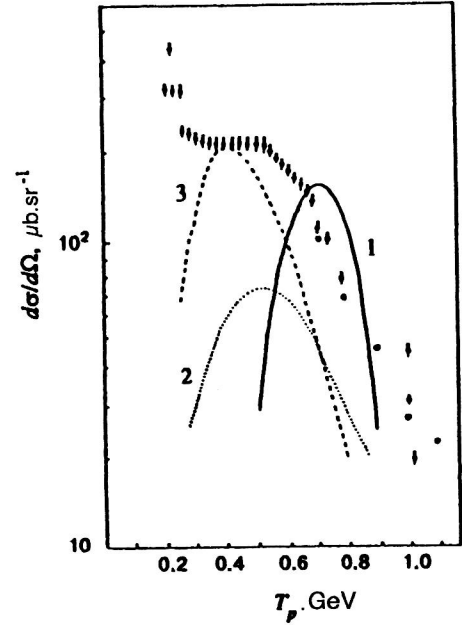


FIG. 5. Contribution of the  $\Delta$ -resonance mechanism to the cross section for backward elastic  $pd$  scattering with various parametrizations of the  $NN \rightarrow N\Delta$  amplitude: (1) parametrization from Ref. 8; (2) parametrization from Ref. 57 neglecting the factor (28) at the  $\pi N\Delta$  vertex; (3) the same as curve 2 but including the factor (28). The points  $\bullet$  are the experimental data.<sup>20</sup>

### 5.4. Results of numerical calculations and discussion

The results of calculating the cross section and deuteron polarization tensor in the process  $pd \rightarrow dp$  using the NE,  $\Delta$ , and SS mechanisms are shown in Figs. 5–9. The parametrization of the  $NN \leftrightarrow N\Delta$  amplitude described in Sec. 4 was used. We see from Figs. 5 and 6 that, in contrast to Ref. 8, the result corresponding to the sum of the amplitudes NE+ $\Delta$ +SS satisfactorily reproduces the dependence of the scattering cross section at angle  $\theta_{c.m.} = 180^\circ$  on the initial

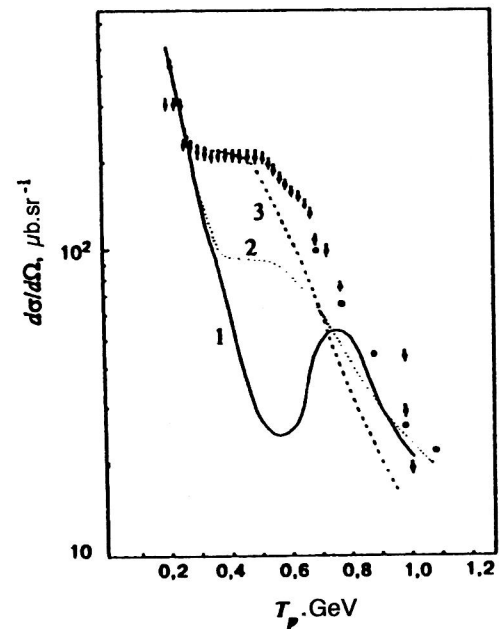


FIG. 6. The same as in Fig. 5, but for the sum of mechanisms NE+ $\Delta$ +SS.

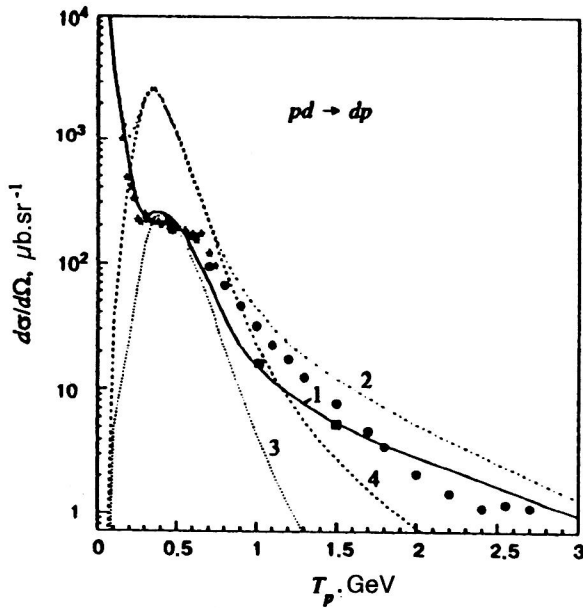


FIG. 7. Differential cross section for backward elastic  $pd$  scattering as a function of the initial energy in the NE+ $\Delta$ +SS model with the form-factor parameters:  $\Lambda_\pi=0.53$  GeV/c,  $\Lambda_\rho=0.7$  GeV/c (solid line);  $\Lambda_\pi=1.3$  GeV/c,  $\Lambda_\rho=1.4$  GeV/c (dot-dash line); the pure contribution of the  $\Delta$  mechanism for these two sets of parameters  $\Lambda_\pi$ ,  $\Lambda_\rho$  is shown by the dotted and dashed lines, respectively. The points are the experimental data of Refs. 20 (\*), 18 (●), and 17 (black squares).

energy in the range 0.2–0.6 GeV without the introduction of any fitted parameters, except those used to describe the  $pp \rightarrow pn\pi^+$  reaction. It should be emphasized that the improvement of the  $NN \leftrightarrow N\Delta$  amplitude compared to Ref. 8

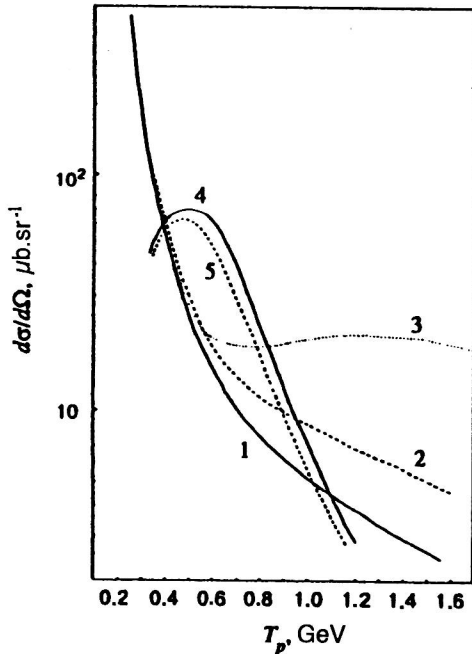


FIG. 8. Calculated contributions of the NE and  $\Delta$  mechanisms to the cross section for backward elastic  $pd$  scattering with various deuteron wave functions: (1) NE with the Paris function; (2) NE with the Ried soft-core function; (3) NE with the Moscow State University function<sup>75</sup>; (4) the  $\Delta$  mechanism with the Paris function; (5) the  $\Delta$  mechanism with the Ried soft-core function.

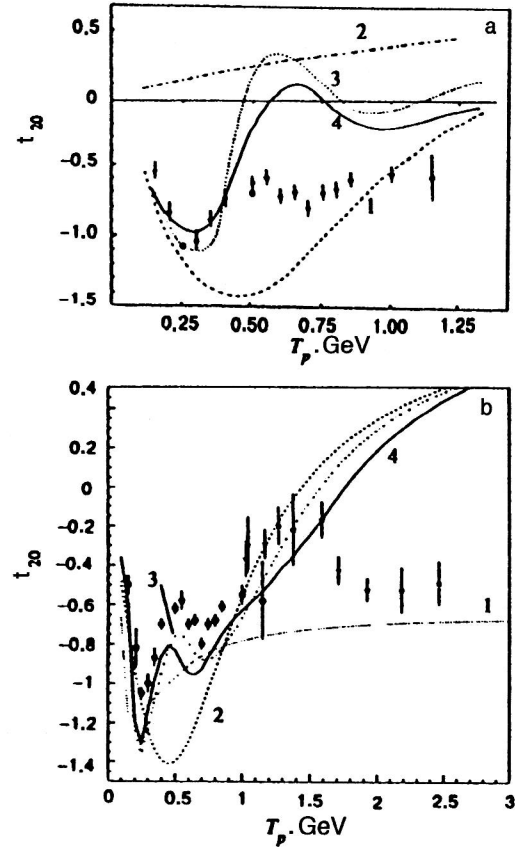


FIG. 9. Deuteron tensor polarization  $t_{20}$  in backward elastic  $pd$  scattering as a function of the initial energy for various mechanisms. (a): (1) NE; (2)  $\Delta$ ; (3) NE+ $\Delta$ +SS; (4) NE+ $\Delta$ +SS+TBR. The curves in (b) were obtained for changed sign of the  $D$  wave [ $w(r) \rightarrow -w(r)$ ] in the  $\Delta$  amplitude: the dotted line is the  $\Delta$ -mechanism contribution, the dashed line is the ONE contribution, the dot-dash line is the  $\Delta$ +ONE contribution, and the solid line is the  $\Delta$ +ONE+SS contribution. The experimental data are from Refs. 19 (●) and 23 (\*).

using the description of the  $pp \rightarrow pn\pi^+$  process in this kinematical region leads directly to an improved description of the experimental data on the  $pd \rightarrow dp$  process. Let us discuss some important features of the NE+ $\Delta$ +SS model.

First, the off-shell behavior of the  $\Delta$  isobar is very important. In the description of the  $pp \rightarrow pn\pi^+$  reaction, the factor  $Z(k)$  defined in (28) is present at the vertex where the virtual  $\Delta$  isobar decays into a real  $\pi$  meson and a nucleon, according to the phenomenology of free  $\pi p$  scattering. The situation regarding the  $pd \rightarrow dp$  process is different. Along with the  $\Delta$  isobar, the  $\pi(\rho)$  meson is also off-shell. Therefore, an ambiguity arises in the calculation of the contribution of the  $\Delta$  mechanism to the  $pd \rightarrow dp$  cross section: it is not clear if the factor  $Z(k)$  should (a) or should not (b) be substituted into the vertex with off-shell  $\pi$  meson and  $\Delta$  isobar. There are no formal arguments favoring either choice, and in both cases roughly identical results of the fit of the cross section for the reaction  $pp \rightarrow pn\pi^+$  are obtained with a slight change in the parameters  $\Lambda_\pi$  and  $\Lambda_\rho$  (Ref. 13). However, in the case of the  $pd \rightarrow dp$  process this ambiguity significantly affects the magnitude of the  $\Delta$ -mechanism contribution. The cross sections calculated with  $Z(k) \neq 1$  and  $Z(k) = 1$  differ by a factor of 2 at the points  $T_p = 0.5$  GeV



and  $T_p = 1$  GeV. The two calculations give the same result at the point  $T_p = 0.7$  GeV, at which the  $\Delta$  isobar is on-shell in this model. For comparison, in Fig. 5 we show the results of calculating the contribution of the  $\Delta$  mechanism with the parameters from Ref. 8. It is clear from our calculations<sup>13</sup> that the maximum in the cross section calculated including only the contribution of the  $\Delta$  mechanism is shifted to lower energies compared to Ref. 8. This is due to the  $k$  dependence of the total  $\Delta$  width in (25). It was assumed in Ref. 8 that the width  $\Gamma$  is independent of  $k$ :  $\Gamma(k) = \Gamma_0 = \text{const}$ . It is not possible to describe the location and height of the experimental maximum in the cross section of the process  $pp \rightarrow pn\pi^+$ , while the pure contribution of the  $\Delta$  mechanism to the  $pd \rightarrow dp$  process near where the  $\Delta$  isobar goes off-shell is overestimated.

Second, an important feature of the NE+ $\Delta$ +SS model is the nature of the interference between the  $\Delta$  and NE mechanisms. In Ref. 8 the total NE+ $\Delta$ +SS contribution in the energy range 0.6–0.8 GeV turned out to be smaller than the contribution of only the  $\Delta$  mechanism and considerably lower than the experimental data. The reason for this destructive interference of the  $\Delta$  and NE mechanisms (the contribution of the SS mechanism is negligible in this region and the interference with it is not important) in Ref. 8 was the large contribution of the  $\rho$  meson to the  $NN \leftrightarrow N\Delta$  amplitude. In the parametrization used in Refs. 57 and 13, the  $\rho$ -meson contribution is minimal, because<sup>2)</sup>  $\Lambda_\rho \sim m_\rho$ . Owing to this, the  $M_{\Delta}^{\pi^+\rho}$ +NE interference is constructive, and the total contribution of the NE+ $\Delta$ +SS mechanism in the range  $T_p = 0.4$ –0.8 GeV in this case proves to be larger than the contribution of the pure  $\Delta$  mechanism and considerably closer to the data than in Ref. 8.

Third, the  $\Delta$  mechanism of the process  $pd \rightarrow dp$  is very sensitive to the parameters of the form factors at the  $\pi NN$ ,  $\pi N\Delta$ ,  $\rho NN$ , and  $\rho N\Delta$  vertices. Our calculations show that the use of the cutoff parameters  $\Lambda_\pi = 1.3$  GeV/ $c$  and  $\Lambda_\rho = 1.4$  GeV/ $c$  given in Ref. 72 leads to a differential cross section in the NE+ $\Delta$ +SS model which is an order of magnitude higher than the experimental data in the range 0.5–1.0 GeV (see Fig. 7).

Fourth, the parameters of the NE+ $\Delta$ +SS model are best justified near where the  $\Delta$  isobar goes on-shell ( $T_p \sim 0.7$  GeV). However, from Fig. 6 we see that at this energy the model gives an absolute value of the experimental cross section too low by a factor of  $\sim 2$ . This disagreement cannot be eliminated by replacing one realistic deuteron wave function by another owing to the weak sensitivity of the  $\Delta$  mechanism to the behavior of the wave function at small internucleon separations. This property of the  $\Delta$  mechanism, the weak sensitivity to the details of the behavior of the deuteron wave function at small  $NN$  separations, is illustrated in Fig. 8, where we give the contributions of the  $\Delta$  and NE mechanisms calculated for various deuteron wave functions, namely, the Paris function,<sup>73</sup> the RSC function,<sup>74</sup> and the Moscow State University function.<sup>75</sup> In the Paris function the high-momentum component is somewhat weaker than in the RSC function. Therefore, for the NE mechanism, which is most sensitive to the high-momentum components of the wave function  $\psi_d(\mathbf{q})$ , the cross section

for the Paris function is smaller in magnitude than that for the RSC function (and significantly smaller than that for the function of Ref. 75). On the other hand, for the  $\Delta$  mechanism the cross section for the Paris function is somewhat larger than for the RSC. This clearly shows that the  $\Delta$  mechanism is important not at small internucleon separations in the deuteron, but rather at intermediate and large ones. The NE mechanism dominates for  $T_p = 0.1$ –0.3 GeV, which follows from the description of the cross section and the deuteron tensor polarization. At energies  $T_p = 0.6$ –1.0 GeV the relative contribution of the NE mechanism is small, but for  $T_p \geq 1.0$  GeV its role is again significant.

The question of the tensor polarization  $t_{20}$  is more complicated. In the region where the NE mechanism dominates ( $T_p \leq 0.2$  GeV), the values of  $t_{20}$  for the NE mechanism agree with experiment (see Fig. 9). For  $T_p \geq 0.25$  GeV the value of  $t_{20}$  predicted by the pure NE mechanism disagrees with the experimental data. The calculations using the one-NE mechanism performed recently in the fully covariant Bethe–Salpeter formalism with the one-boson exchange potential in the ladder approximation<sup>35</sup> do not improve the agreement with experiment for  $t_{20}$ . Inclusion of the  $\Delta$ -mechanism contribution restores the agreement at fairly low energies  $T_p = 0.25$ –0.4 GeV. However, at higher energies  $T_p \geq 0.4$  GeV the value  $t_{20} = -0.2$ – $+0.2$  predicted by the NE+ $\Delta$ +SS model is in sharp contradiction with the data. As in Ref. 8, here the values of  $t_{20}$  are positive for the  $\Delta$  mechanism. Using the same spin structure of the  $NN \leftrightarrow N\Delta$  amplitude as used here in Eq. (30), the authors of Ref. 12 obtained  $t_{20} \sim -0.5$ , which is considerably closer to experiment. However, in their calculation<sup>12</sup> of the  $\Delta$  amplitude, the  $\Delta$  propagator was taken outside the integral over the intermediate nucleon momenta. According to estimates<sup>76</sup> made for the deuteron  $S$  wave, this approximation reduces the contribution of the  $\Delta$  mechanism by a factor of 2 to 3. This underestimate is then artificially compensated for<sup>12</sup> by a special choice of the parameters of the  $NN \leftrightarrow N\Delta$  amplitude, in contradiction with the experimental data on the  $pp \rightarrow pn\pi^+$  cross section. When the deuteron  $D$  wave is included within the approximations used in Ref. 12, a different spin structure of the amplitude  $M^{(\Delta)}$  arises compared with the calculation of Refs. 8 and 76. In connection with this, we note that our analysis shows that when the contribution of the deuteron  $D$  wave is excluded from the  $\Delta$  amplitude of Ref. 8, the value of  $t_{20}$  becomes negative, while when the sign is changed in (38),  $w(r) \rightarrow -w(r)$ , qualitative agreement with the data is obtained (see Fig. 9a).<sup>3)</sup> Therefore, to reach a more definite conclusion about the value of  $t_{20}$  in the NE+ $\Delta$ +SS model, it is important to keep not only the  $\Delta$ -isobar propagator, but also the  $\pi NN$  and  $\pi N\Delta$  vertex functions inside the integral in the  $\Delta$  amplitude. This technically complicated problem has not yet been solved. In addition, it may prove important to include  $\sigma$  and  $\omega$  exchange in the  $NN \rightarrow N\Delta$  amplitude, because the polarization characteristics of the reaction  $pp \rightarrow pn\pi^+$  cannot be described using only  $\pi + \rho$  exchange.<sup>60</sup>

We note that the disagreement between the predictions of the NE+ $\Delta$ +SS model and experiment occurs both for the spin-averaged cross section and for  $t_{20}$  at  $T_p \geq 0.4$  GeV. As

shown in Ref. 13, the inclusion of three-baryon resonances, the possible existence of which was first mentioned in Ref. 8, does not improve the agreement with experiment for  $t_{20}$  even with the most general assumptions about the spin structure of the corresponding amplitude. In Sec. 6 we shall discuss a possible connection between this disagreement and the  $N^*$ -isobar exchange mechanism due to the admixture of  $NN^*$  components in the deuteron. According to estimates,<sup>28</sup> the maximum contribution of  $N^*$  exchange is expected to occur in the energy range  $T_p = 0.5\text{--}1.0$  GeV.

### 5.5. The role of the three-baryon resonance mechanism

One possible way of overcoming the disagreement between the  $NE + \Delta + SS$  model and the spin-averaged cross section for the process  $pd \rightarrow dp$  is to include the contribution of the three-baryon resonance (TBR) mechanism. The idea of such a mechanism was first mentioned in Ref. 8. It was later shown<sup>77</sup> that this idea is consistent with the experimental data on the cross section ratio  $R = d\sigma(p, nd)/d\sigma(p, pd)$  for the nuclei  ${}^6, {}^7\text{Li}$  at 670 MeV. The possible existence of three-baryon resonances is predicted in the model of elongated rotating bags with hidden color.<sup>53</sup> If we assume that the entire disagreement between the experimental data on the spin-averaged cross section of the process  $pd \rightarrow dp$  and the  $NE + \Delta + SS$  model is due to the contribution of three-baryon resonances, we can obtain an upper limit on the TBR contribution. This was done in Ref. 8. This result now needs to be reevaluated, as in Ref. 13 we obtained a  $\Delta$ -mechanism contribution different from that of Ref. 8. Moreover, the TBR amplitude averaged over proton spins was used in Ref. 8. We shall take into account the spin structure of the TBR amplitude more accurately, using for it the expression<sup>13</sup>

$$A_{\text{TBR}} = \langle \sigma'_p \lambda'_d | T | \sigma_p \lambda_d \rangle = \sum_{SL'S'L'M} \frac{G^2}{E - M_0 + i\Gamma/2} \times (-1)^{L'} \sqrt{(2L+1)(2L'+1)} \left( 1\lambda_d \frac{1}{2} \sigma_p \middle| SM_S \right) \times (LOS M_S | JM) \left( 1\lambda'_d \frac{1}{2} \sigma'_p \middle| S' M'_S \right) \times (L' 0 S' M'_S | JM), \quad (47)$$

where  $L$  ( $L'$ ) and  $S$  ( $S'$ ) are the orbital angular momentum and spin of the channel  $p + d$  ( $p' + d'$ ),  $J$  is the total angular momentum of the TBR,  $\Gamma$  is its width,  $M_0$  is its mass, and  $G$  is the coupling constant at the  $p + d \leftrightarrow 9q$  vertex.

The calculations were carried out assuming that  $L = L'$  and  $S = S'$ . As in Ref. 8, here it is assumed that only the three resonances decaying into the  $D$ ,  $F$ , and  $G$  states of the  $pd$  system give the largest contribution. The resonance parameters are found by a fit to the experimental data:  $M \sim 3.1\text{--}3.2$  GeV,  $\Gamma \sim 100\text{--}200$  MeV, and  $G \sim 0.3\text{--}0.7$ . Equation (47) reduces to (11) from Ref. 52 only in the limit  $S_d \gg S_p$ . Using (47), we find that for the three TBR amplitudes considered,  $t_{20}$  lies in the range  $t_{20}^{\text{TBR}} = -0.4\text{--}+0.4$ , including the point  $t_{20} = 0$ . However, even in the most favorable case ( $t_{20} = -0.4$ ), for the total  $NE + \Delta + SS + \text{TBR}$

amplitude the calculated value of  $t_{20}$  is close to zero for  $T_p > 0.6$  GeV, i.e., much higher than the experimental points.

It can therefore be concluded that the role of the TBR mechanism is greatly exaggerated in Refs. 8 and 52, especially in the interpretation of  $t_{20}$ . However, at present there is no justification for completely discarding this mechanism. The question of the role of the TBR mechanism in  $t_{20}$  should be reexamined after calculating the contribution of the  $\Delta$  mechanism more accurately and performing a complete polarization experiment.<sup>22</sup>

## 6. $N^*$ -ISOBAR EXCHANGE AND THE ROLE OF RESCATTERINGS

### 6.1. The one-boson exchange mechanism in relativistic dynamics

In this section we give the expressions for the baryon-exchange mechanism obtained earlier<sup>6,8</sup> including only the  $p + n$  component of the deuteron, and then generalized<sup>28</sup> to the case of nucleon isobar  $N^*$  exchange in the process  $pd \rightarrow dp$  and neutron exchange in the process  $pd \rightarrow dN^*$  (Ref. 78).

**The BKT approach.** Our discussion is based on that of Bakker, Kondratyuk, and Terentjev<sup>36</sup> (BKT), who constructed Faddeev-type equations for the three-body problem in relativistic dynamics. The advantage of this approach is that the commutation relations for the Poincaré generators of the three-body system, and, in particular, the angular condition, are satisfied exactly. Without dwelling on the technical details of the approach,<sup>36</sup> let us give the final expression for the amplitude of the process  $p_i d \rightarrow dp_f$  within the one-boson exchange (OBE) mechanism (see Figs. 1b and 1f):

$$A_{\text{OBE}}^{\text{BKT}} = K \sum_{|N\rangle} \{ \Psi_{\lambda_f}^{\sigma_i \sigma_N}(\mathbf{q}_i) \}^+ \Psi_{\lambda_i}^{\sigma_i \sigma_N}(\mathbf{q}_f), \quad (48)$$

where

$$K = \begin{pmatrix} 2 \\ 1 \end{pmatrix} 2 \sqrt{E_{d_i}(E_{p_i} + E_N) E_{d_f}(E_{p_f} + E_N)} \frac{\sqrt{s} - M_0}{E_N} \quad (49)$$

is a kinematical factor and  $\Psi_{\lambda_d}^{\sigma_p \sigma_N}(\mathbf{q})$  is the deuteron wave function in the channel  $d \rightarrow p + N$  (an eigenfunction of the mass operator of the  $p + N$  system). Its normalization condition is

$$\frac{1}{2J_d + 1} \sum_{\lambda_d, \sigma_p, \sigma_N} \int |\Psi_{\lambda_d}^{\sigma_p, \sigma_N}(\mathbf{q})|^2 \kappa_{pN}^{-1}(q) \frac{d^3 q}{(2\pi)^3} = N_d^{pN}, \quad (50)$$

where

$$\kappa_{pN}(q) = \frac{2\varepsilon_p(q)\varepsilon_N(q)}{\varepsilon_p(q) + \varepsilon_N(q)}, \quad \varepsilon_j(\mathbf{q}) = \sqrt{m_j^2 + \mathbf{q}_j^2}, \quad (51)$$

$N_d^{pN}$  is the effective number for the corresponding  $p + N$  component of the deuteron and includes the squared isotopic Clebsch–Gordan coefficient,  $(\frac{1}{2}\tau_p \frac{1}{2}\tau_N | 00)^2 = \frac{1}{2}$ , so that, for example, for the  $p + n$  component of the deuteron we have  $N_d^{pN} = 0.5$ . Equation (48) includes the combinatorial factor  $\binom{2}{1} = 2$ , because the 6-quark deuteron function used here is

completely antisymmetric in the quarks;  $\sigma_i$  ( $\sigma_f$ ) and  $\sigma_N$  are the spin projections of the initial (final) nucleon and the transferred baryon, respectively; and  $\lambda_i$  ( $\lambda_f$ ) is the spin projection of the initial (final) deuteron. We have used the following notation in (49) and (51):  $E_k(\mathbf{p}_k) = \sqrt{m_k^2 + \mathbf{p}_k^2}$  and  $\mathbf{p}_k$  are the energy and momentum of the  $k$ th particle ( $k = p_i, p_f, N, d_i, d_f$ ) in the 3-body c.m. frame of  $p_i + d = p_f + d$ ;  $\varepsilon_j(\mathbf{q}) = \sqrt{m_j^2 + \mathbf{q}^2}$  and  $\mathbf{q}$  are the energy and momentum of the  $j$ th particle ( $j = p_i, p_f, N$ ) in the 2-body c.m. frame of  $p_i + N$  or  $p_f + N$ ;  $\sqrt{s}$  is the invariant mass of the system  $p_i + d = p_f + d$ , and  $M_0 = E_N + E_{p_i} + E_{p_f}$  is the mass of the intermediate state. In (48) we sum over the internal states of the transferred baryon  $N$  (a neutron or nucleon resonance), including its spin projection  $\sigma_N$ . The arguments of the wave functions of the initial and final deuterons  $\mathbf{q}_i$  and  $\mathbf{q}_f$  are expressed in terms of the momenta and energies of the observed particles using Eq. (2) as

$$\mathbf{q}_i = \frac{(\varepsilon_N + E_N)\mathbf{p}_i - (\varepsilon_{p_i} + E_{p_i})\mathbf{p}_N}{\varepsilon_N + E_N + \varepsilon_{p_i} + E_{p_i}}, \quad \varepsilon_N \equiv \varepsilon_N(\mathbf{q}_i),$$

$$\varepsilon_{p_i} \equiv \varepsilon_{p_i}(\mathbf{q}_i) \quad (52)$$

$$\mathbf{q}_f = \frac{(\varepsilon_N + E_N)\mathbf{p}_f - (\varepsilon_{p_f} + E_{p_f})\mathbf{p}_N}{\varepsilon_N + E_N + \varepsilon_{p_f} + E_{p_f}}, \quad \varepsilon_N \equiv \varepsilon_N(\mathbf{q}_f),$$

$$\varepsilon_{p_f} \equiv \varepsilon_{p_f}(\mathbf{q}_f). \quad (53)$$

The 3-momentum of the transferred nucleon  $N$  in (52) and (53) is related to the 3-momenta of the initial and final particles in the  $p + d$  c.m. frame as<sup>36</sup>

$$\mathbf{p}_N = \mathbf{p}_{d_i} - \mathbf{p}_f = \mathbf{p}_{d_f} - \mathbf{p}_i, \quad (54)$$

The squared modulus of the amplitude (48) averaged over the spins of the initial particles and summed over the spins of the final particles is related to the differential cross section of the process  $pd \rightarrow pd$  in the  $p + d$  c.m. frame as

$$\frac{d\sigma}{d\Omega} = \frac{1}{64\pi^2 s} |A_{\text{OBE}}|^2. \quad (55)$$

**Noncovariant light-cone dynamics.** Let us consider the one-nucleon exchange amplitude for the process  $pd \rightarrow dp$  using noncovariant light-cone dynamics (LCD) without the three-particle angular condition. This approach has been used in Refs. 5, 6, and 11. Even though the results are rather applied (see Ref. 79 and references therein), we shall give them here only for comparison with the OBE mechanism in the BKT approach, in which the rotational invariance is not violated.

Using the properties of the nucleon  $|\mathbf{p}_\perp, p^+\rangle$  and deuteron  $|\mathbf{d}_\perp, d^+\rangle$  free states in LCD and taking into account the conservation of the  $p^+$  and  $\mathbf{p}_\perp$  components of the 4-momenta at the  $d \rightarrow p_f + N$  and  $p_i + N \rightarrow d$  vertices, for the OBE amplitude in the noncovariant form of LCD we obtain

$$A_{\text{OBE}}^{\text{LCD}} = \begin{pmatrix} 2 \\ 1 \end{pmatrix} \frac{1}{1 - \xi'} [m_d^2 - M_i^2(\mathbf{k}_\perp, \xi)]$$

$$\times \sum_{\sigma_N} \{ \Psi_{\lambda_f}^{\sigma_i \sigma_N}(\mathbf{k}'_\perp, \xi') \} + \Psi_{\lambda_i}^{\sigma_f \sigma_N}(\mathbf{k}_\perp, \xi) \}, \quad (56)$$

where  $\Psi_d(\mathbf{k}_\perp, \xi)$  is the deuteron wave function (i.e., the eigenfunction of the squared mass operator  $\hat{M}^2$  with eigenvalue  $m_d^2$ ), which is related to the wave function in (48)  $\Psi_{\lambda_d}^{\sigma_p, \sigma_N}(\mathbf{q})$  by the Melosh transformation.<sup>80</sup>

In (56) the internal LCD variables  $\mathbf{k}_\perp$ ,  $\xi$ ,  $\mathbf{k}'_\perp$ , and  $\xi'$  are related to the one-particle external variables by relations expressing the conservation of the  $p^+$  and  $\mathbf{p}_\perp$  components of the 4-momenta at the  $d \leftrightarrow N + N$  vertices. In the noncovariant LCD approach the wave functions  $\Psi_{d_i}$  and  $\Psi_{d_f}$  depend only on the squared modulus of the relative momentum  $k^2$ , which is uniquely related to the invariant masses  $M_f^2 = M^2(\mathbf{k}'_\perp, \xi')$  and  $M_i^2 = M^2(\mathbf{k}_\perp, \xi)$  of the free pairs  $p_i + N$  and  $p_f + N$ , respectively. The violation of rotational invariance in the noncovariant LCD approach is manifested in the dependence of the arguments  $k_i^2$  and  $k_f^2$  of the wave functions of the initial and final deuterons on the direction of the  $OZ$  axis. In Ref. 6 the  $OZ$  axis was chosen such that  $OZ \uparrow \mathbf{p}_{p_i} + \mathbf{p}_{p_f}$ . This choice ensures symmetry of the initial and final protons (deuterons):  $\xi = \xi'$  and  $\mathbf{k}_\perp^2 = \mathbf{k}'_\perp^2$ . This symmetry is preserved in  $N^*$  exchange. However, in the case of the reaction  $pd \rightarrow dN^*$ , the choice of a particular direction of the  $OZ$  axis is difficult to justify on the basis of symmetry requirements or minimization of the contribution of multiparticle intermediate states, as was done in Ref. 6. Therefore, in Ref. 78 the reaction  $pd \rightarrow dN^*$  is studied only in the BKT approach.

## 6.2. The inclusion of rescattering in the initial and final states

Repeating the arguments of Ref. 27, where the two-nucleon transfer mechanism in the process  $p + {}^3\text{He} \rightarrow {}^3\text{He} + p$  was studied, for the nucleon-exchange amplitude in the process  $pd \rightarrow dp$  taking into account rescatterings (distortions) in the initial and final states we find

$$T_{\text{NE}}^{\text{dist}} = T_B(\mathbf{d}_f, \mathbf{p}_f; \mathbf{d}_i, \mathbf{p}_i)$$

$$+ \frac{i}{4\pi p_i} \int d^2 q F_{pd}(\mathbf{q}) T_B(\mathbf{d}_f, \mathbf{p}_f; \mathbf{d}_i + \mathbf{q}, \mathbf{p}_i - \mathbf{q})$$

$$+ \frac{i}{4\pi p_f} \int d^2 q' f_{pp}(\mathbf{q}') T_B(\mathbf{d}_f - \mathbf{q}', \mathbf{p}_f + \mathbf{q}'; \mathbf{d}_i, \mathbf{p}_i)$$

$$- \frac{1}{(4\pi)^2 p_f p_i} \int \int d^2 q d^2 q' F_{pd}(\mathbf{q}) f_{pp}(\mathbf{q}') T_B(\mathbf{d}_f$$

$$- \mathbf{q}', \mathbf{p}_f + \mathbf{q}; \mathbf{d}_i + \mathbf{q}, \mathbf{p}_i - \mathbf{q}). \quad (57)$$

Here  $\mathbf{p}_i$  ( $\mathbf{d}_i$ ) is the momentum of the initial proton (deuteron) in the  $p + d$  c.m. frame and  $\mathbf{p}_f$  ( $\mathbf{d}_f$ ) is the momentum of the final proton (deuteron); the integration variables  $\mathbf{q}$  and  $\mathbf{q}'$  in (57) are the 2-dimensional momenta transferred in  $pd$  and  $pp$  rescatterings, respectively; the amplitude of elastic  $pN$

scattering,  $f_{pN}$ , for which we use the spinless approximation, is parametrized in the form standard for diffraction theory.<sup>81</sup>

$$f_{pN}(q) = \frac{k\sigma_{pN}}{4\pi} (i + \alpha_{pN}) \exp\left(-\frac{1}{2} \beta_{pN} q^2\right), \quad (58)$$

where  $q$  is the momentum transfer,  $k$  is the nucleon wave vector in the  $p + N$  c.m. frame,  $\sigma_{pN}$  is the total cross section of  $pN$  scattering,  $\alpha_{pN}$  and  $\beta_{pN}$  are empirical parameters corresponding to the experimental data on  $pN$  scattering, and  $F_{pd}(q)$  is the amplitude of forward elastic  $pd$  scattering, here calculated using Glauber–Sitenko multiple scattering theory.<sup>81</sup> The Born amplitude  $T_B$  is related to the invariant amplitude  $A$  in (48) as

$$A_{NE} = 4m_p m_d T_B. \quad (59)$$

In deriving the amplitude of forward elastic  $pd$  scattering in the Glauber–Sitenko theory, the integration over the 2-dimensional momentum transferred to the nucleons is performed in the plane perpendicular to the eikonal axis, which is taken to lie along the vector  $\mathbf{p}_i + \mathbf{p}_f$ , i.e., along the bisector of the angle between the momenta of the initial and final protons. As is well known (see, for example, Ref. 82), this approximation works well for scattering into the forward hemisphere. Accordingly, in the integration over  $d^2q$  and  $d^2q'$  in (57) it is necessary to take the eikonal axis to lie along the vector  $\mathbf{p}_i - \mathbf{p}_f$ , which corresponds to small  $pp$ - and  $pd$ -rescattering angles  $\tilde{\theta} = \pi - \theta_{c.m.}$ , where  $\theta_{c.m.}$  is the scattering angle in the process  $pd \rightarrow dp$ , close to  $180^\circ$ . Obviously, if the Glauber–Sitenko approximation for the forward  $pd$ -scattering amplitude  $F_{pd}$  works well for small angles in the range  $0 - \tilde{\theta}_{\max}$ , then the formalism used here to include rescattering in the process  $pd \rightarrow dp$  should work in the corresponding range of large backward  $pd$ -scattering angles  $\theta_{c.m.} = [\pi - \tilde{\theta}_{\max}, \pi]$ .

Let us discuss the expressions for the arguments of the deuteron wave functions in (57), shown graphically in Fig. 10, denoting the momenta for the second, third, and fourth terms by the superscripts  $k=2,3$ , and 4:

$$\begin{aligned} T_B &\sim \psi_{d_i}\left(\mathbf{q}_i = \frac{1}{2} \mathbf{d}_f - \mathbf{p}_i\right) \psi_{d_f}^*\left(\mathbf{q}_f = \frac{1}{2} \mathbf{d}_i - \mathbf{p}_f\right); \\ T^{(2)} &\sim \int d^2q \psi_{d_i}(\mathbf{Q}_i^{(2)} = \mathbf{q}_i + \mathbf{q}) \psi_{d_f}^*(\mathbf{Q}_f^{(2)} = \mathbf{q}_f + \frac{1}{2} \mathbf{q}); \\ T^{(3)} &\sim \int d^2d' \psi_{d_i}(\mathbf{Q}_i^{(3)} = \mathbf{q}_i - \frac{1}{2} \mathbf{q}') \psi_{d_f}^*(\mathbf{Q}_f^{(3)} = \mathbf{q}_f - \mathbf{q}'); \\ T^{(4)} &\sim \int \int d^2q d^2q' \psi_{d_i}(\mathbf{Q}_i^{(4)} = \mathbf{q}_i + \mathbf{q} - \frac{1}{2} \mathbf{q}') \\ &\quad \times \psi_{d_f}^*(\mathbf{Q}_f^{(4)} = \mathbf{q}_f + \frac{1}{2} \mathbf{q} - \mathbf{q}'). \end{aligned} \quad (60)$$

It follows from these expressions that for the scattering angle  $\theta_{c.m.} = 180^\circ$  ( $\mathbf{q} \perp \mathbf{q}_i$ ,  $\mathbf{q} \perp \mathbf{q}_f$ ) the momentum transfer in rescattering increases the moduli  $|\mathbf{Q}_i^{(k)}|$  and  $|\mathbf{Q}_f^{(k)}|$ ,  $k=2,3,4$ . On the other hand, at  $\theta_{c.m.} < 180^\circ$ , for all three terms involving rescattering there exists a range of the arguments  $\mathbf{q}$  and  $\mathbf{q}'$  in

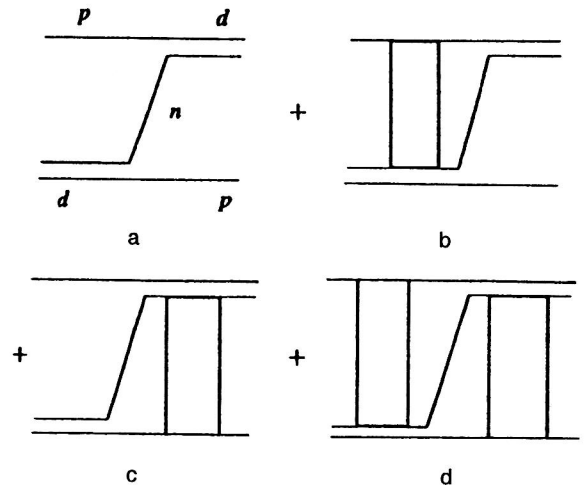


FIG. 10. Mechanism of one-nucleon exchange with rescattering: (a) neutron exchange in the Born approximation; (b) neutron exchange with  $pd$  rescattering; (c) neutron exchange with  $pp$  rescattering; (d) neutron exchange with  $pp + pd$  rescattering.

which the moduli  $|\mathbf{Q}_i^{(k)}|$  and  $|\mathbf{Q}_f^{(k)}|$  are decreased compared to the values  $|\mathbf{q}_i|$  and  $|\mathbf{q}_f|$  characteristic at the given scattering angle  $\theta_{c.m.}$  in the Born approximation. This region can give the dominant contribution to the integrals over  $d^2q$  and  $d^2q'$ , because the wave function  $\psi_d(\mathbf{q})$  grows rapidly as its argument decreases. The moduli  $|\mathbf{Q}_i^{(k)}|$  and  $|\mathbf{Q}_f^{(k)}|$  decrease owing to the cancellation of their transverse components  $|\mathbf{Q}_{i\perp}^{(k)}|$  and  $|\mathbf{Q}_{f\perp}^{(k)}|$  lying in the plane of the vectors  $\mathbf{q}$  and  $\mathbf{q}'$ . This effect is larger the more rapidly the wave function  $\Psi_d(\mathbf{Q})$  falls off with increasing relative momentum  $Q$  and the more slowly the amplitudes  $f_{pp}(q)$  and  $F_{pd}(q)$  fall off with increasing momentum transfer  $q$ . This can be clearly seen from the explicit analytic expressions for the amplitudes of NE with rescattering if the deuteron wave function is taken to be an expansion in Gaussians:  $\psi_S(q) = \sum_j A_j \times \exp(-\gamma_j q^2)$ . For example, in the  $S$ -wave approximation for the deuteron wave function (in actual calculations both the  $S$  and  $D$  components of the wave function are included) the NE amplitude with  $pp$  rescattering in the final state has the form

$$\begin{aligned} T_S^{(3)}(\mathbf{q}_i, \mathbf{q}_f) &= \frac{-i}{4\pi p_i} \sum_{j,k} a_{pp} A_k A_j \frac{\pi}{Y} \exp[-(\gamma_k q_f^2 + \gamma_j q_i^2)] \\ &\quad \times \exp\left[\frac{(2\gamma_k \mathbf{q}_{f\perp} + \gamma_j \mathbf{q}_{i\perp})^2}{Y}\right] \left[\varepsilon_d + \frac{q_i^2}{m_p}\right. \\ &\quad \left. - \frac{1}{2m_p Y} (2\gamma_k \mathbf{q}_{f\perp} + \gamma_j \mathbf{q}_{i\perp}) \mathbf{q}_{i\perp}\right. \\ &\quad \left. + \frac{1}{16m_p Y^2} (2\gamma_k \mathbf{q}_{f\perp} + \gamma_j \mathbf{q}_{i\perp})^2 + \frac{1}{4m_p Y}\right]. \end{aligned} \quad (61)$$

Here  $\beta_{pp}$  and  $a_{pp} = \sigma_{pp}(i + \alpha_{pp})/4\pi$  are the parameters of the  $pp$  scattering amplitude (58);  $Y = \beta_{pp} + \gamma_k + \frac{1}{4}\gamma_j$ ; and the transverse components of the momenta  $\mathbf{q}_{i\perp}$  and  $\mathbf{q}_{f\perp}$  are perpendicular to the direction of the eikonal axis, which lies along the vector  $(\mathbf{p}_i - \mathbf{p}_f)$ . The first exponential factor with negative argument in (61) leads to “normal” falloff of the



amplitude of the process with increasing “Born” momenta  $q_i$  and  $q_f$ . The second exponential with positive argument in (61) slows down the falloff of the angular dependence. Therefore, the terms with rescattering at  $\theta_{\text{c.m.}} < 180^\circ$  can prove more important than the first Born term.

### 6.3. The spin structure of the OBE amplitude

**The  $p+n$  component.** The spin structure of the Born amplitude of neutron exchange for the  $p+n$  component of the deuteron taking into account the  $S$  and  $D$  waves is well known (see, for example, Refs. 4 and 8).

**The  $p+N^*$  component.** According to calculations<sup>1</sup> based on the Regge model and an analysis<sup>83</sup> using the theory of meson exchange, the contribution of the  $NN^*$  components is important for understanding the experimental data on the cross section for backward  $pd$  scattering at energies  $\sim 1$  GeV. However, the use of the Regge model at energies of the order of the nucleon mass and also the significant uncertainties in the information about the meson– $N$ – $N^*$  vertices make these estimates unreliable. The 6-quark model of the deuteron<sup>84–86</sup> developed later on allows a new approach to the calculation of  $dNN^*$  vertices. In this model the structure of the deuteron at small  $NN$  separations  $r_{NN} \leq 1$  F is determined by the superposition of the unexcited  $s^6$  and excited  $s^4p^2 - s^5s$  quark shell configurations. According to this model, the presence of two-quantum  $2\hbar\omega$  excitations in the  $s^4p^2 - s^5s$  configuration gives rise to a phenomenological repulsive core in the  $NN$  interaction potential.<sup>84,85</sup> This excited quark configuration leads to an admixture of small  $NN^*$  components in the deuteron wave function. The effective numbers and momentum distributions for various baryon–baryon components in the deuteron have been calculated in this approach,<sup>87</sup> which makes it possible to analyze the role of the  $NN^*$  components in the reaction  $dA \rightarrow p(0^\circ)X$  (Refs. 79 and 24).

Let us consider the exchange of nucleon resonances  $N^*$  starting from the  $p+N^*$  component of the deuteron wave function constructed in Refs. 87 and 79. In the quark model the deuteron wave function in the  $d \rightarrow N+B$  channel,  $\Psi_\lambda^{\sigma_N \sigma_B}$ , entering into (48), (50), and (56) is determined by the following overlap integral of the 6-quark wave function of the deuteron  $\Psi_{6q}$  and the product of baryon internal wave functions  $\varphi_N$  and  $\varphi_B$ :

$$\Psi_\lambda^{\sigma_N \sigma_B} = \left( \frac{6!}{3!3!2} \right)^{1/2} \langle \varphi_N \varphi_B | \Psi_{6q} \rangle. \quad (62)$$

The state of a baryon in the quark model is written as an expansion in the basis states of the translationally-invariant shell model. Using the formalism developed<sup>87</sup> for the overlap integrals (62), we obtain the following expression for the amplitude of  $N^*$ -resonance transfer in the process  $pd \rightarrow dp$ :

$$\begin{aligned} A_{\text{OBE}}^{\text{Born}} &= K \sqrt{\kappa_{pN}(q_i) \kappa_{pN}(q_f)} \\ &\times \sum_{\substack{M_{L_B} M_{S_B} \\ M_{L_B}' M_{S_B}' M_{J_B}}} (L_B M_{L_B} S_B M_{S_B} | J_B M_{J_B}) \\ &\times (S_B M_{S_B} 1/2 \sigma_f | 1 \lambda_i) (L_B M_{L_B}' S_B M_{S_B}' | J_B M_{J_B}) \\ &\times (S_B M_{S_B}' 1/2 \sigma_i | 1 \lambda_f) Y_{L_B M_{L_B}}(\hat{\mathbf{q}}_f) Y_{L_B M_{L_B}'}^*(\hat{\mathbf{q}}_i) \\ &\times (\hat{\mathbf{q}}_i) 2 \Phi_{N_B L_B}^2(q_f). \end{aligned} \quad (63)$$

Here  $L_B$ ,  $S_B$ , and  $J_B$  are the orbital angular momentum, the spin, and the total angular momentum of the isobar,  $M_{L_B}$ ,  $M_{S_B}$ , and  $M_{J_B}$  are the corresponding  $z$  projections of these angular momenta, and  $\Phi_{N_B L_B}(q)$  is the wave function of the relative motion in the  $d \rightarrow p+N^*$  channel, normalized by the condition

$$\int_0^\infty \Phi_{N_B L_B}^2(q) q^2 \frac{dq}{(2\pi)^3} = N_d^{pN^*}, \quad (64)$$

where  $N_d^{pN^*}$  is the effective number of  $N^*$  isobars in the deuteron.

The authors of Refs. 87 and 79 used the angular-momentum coupling scheme ( $\mathbf{L}_B + \mathbf{S}_B = \mathbf{J}_B$ ,  $\mathbf{S}_B + \mathbf{s}_p = \mathbf{J}_d$ ) in which the internal orbital angular momentum of the baryon  $B$  is also the orbital angular momentum of the relative motion in the  $d \rightarrow p+B$  channel. Equation (63) was obtained using this coupling scheme. However, in the principal  $d \rightarrow p+n$  channel, which in Refs. 87 and 79 is not described by the quark model, the coupling scheme is different:  $\mathbf{s}_n + \mathbf{s}_p = \mathbf{S}$ ,  $\mathbf{L} + \mathbf{S} = \mathbf{J}_d$ . Therefore, to make the spin structure of the  $pN^*$  component consistent with the spin structure of the  $pn$  component, it is necessary to use the following coupling scheme in the  $d \rightarrow p+B$  channel:

$$\mathbf{L}_B + \mathbf{S}_B = \mathbf{J}_B, \quad \mathbf{J}_B + \mathbf{s}_p = \mathbf{S}, \quad \mathbf{L} + \mathbf{S} = \mathbf{J}_d, \quad (65)$$

where the angular momentum  $L$  has the same parity as  $L_B$  and is here taken equal to  $L_B$ .

### 6.4. Numerical results

**Nucleon resonance exchange.** In the calculation of the contribution of nucleon resonance exchange to the process  $pd \rightarrow dp$ , we included the ten states of the translationally-invariant shell model, given in Table 2 of Ref. 79, for which the effective numbers are at least  $10^{-5}$ . In our calculations the mass of a state was identified with the mass of the resonance in whose wave function the state in question of the translationally-invariant shell model has the largest weight. For example, the state  $|2(20)[21]0\frac{1}{2}\frac{1}{2}\rangle$  is assigned the mass 1710 MeV. The results of the calculations taking into account nucleon resonance exchange are given in Figs. 11–13. The calculations show that the contribution of  $N^*$  exchange depends strongly on the form of relativistic dynamics used. For example, in going from the BKT approach to the noncovariant LCD approach, the contribution of  $N^*$  exchange decreases owing to the increased relative momentum at the

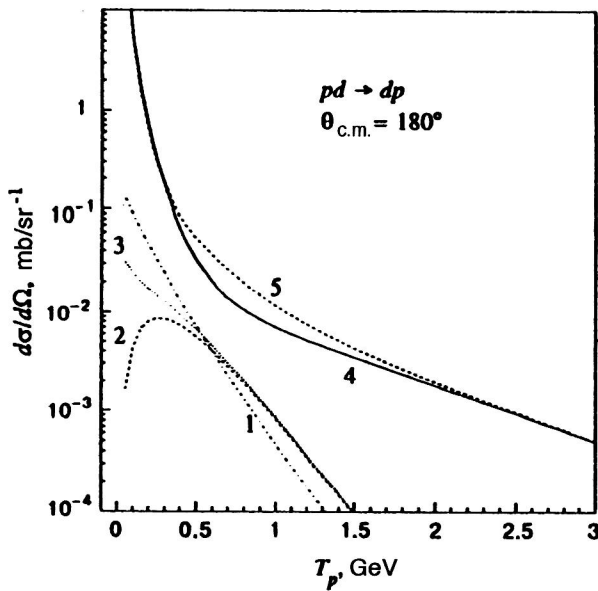


FIG. 11. Calculated cross section for the process  $pd \rightarrow dp$  at  $\theta_{c.m.} = 180^\circ$  as a function of the kinetic energy of the initial proton in the lab frame  $T_p$  for OBE mechanisms: (1) contribution of exchange of  $N^*$  isobars with positive and (2) negative parity; (3) total contribution of  $N^*$  exchange; (4, solid line) neutron exchange, (5) coherent sum of  $n$  and  $N^*$  exchange.

$d \rightarrow NN^*$  vertex. As the mass of the transferred resonance increases, its contribution to the process  $pd \rightarrow dp$  also decreases, because the relative momentum at the  $d \rightarrow NN^*$  vertex is increased. We see from Fig. 11 that the total contribution of negative-parity states, i.e.,  $p$  states of the relative motion in the channel  $d \rightarrow p + N^*$ , is a maximum for initial proton energies in the lab frame  $T_p \sim 0.3$  GeV. The maximum relative contribution of positive-parity resonances, i.e.,  $s$  states of the relative  $p - N^*$  motion in the  $d \rightarrow p + N^*$

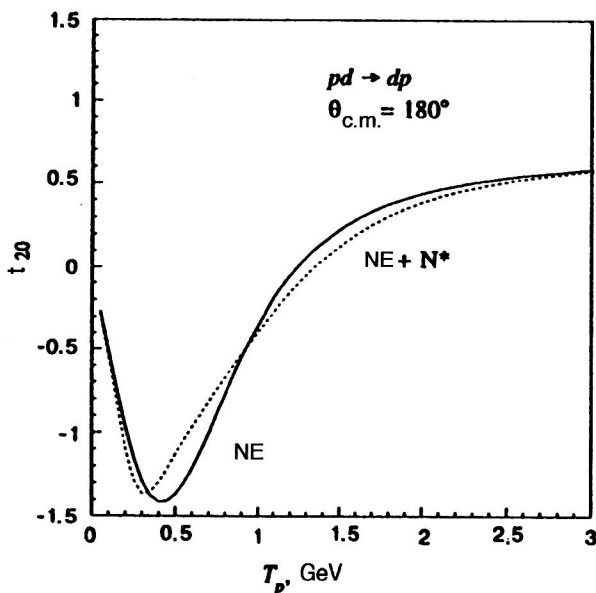


FIG. 12. Calculated deuteron tensor polarization in the process  $pd \rightarrow dp$  at  $\theta_{c.m.} = 180^\circ$  as a function of the incident proton kinetic energy in the lab frame  $T_p$  for OBE mechanisms: the solid line is for NE and the dashed line is the coherent sum of  $n$  and  $N^*$  exchanges.

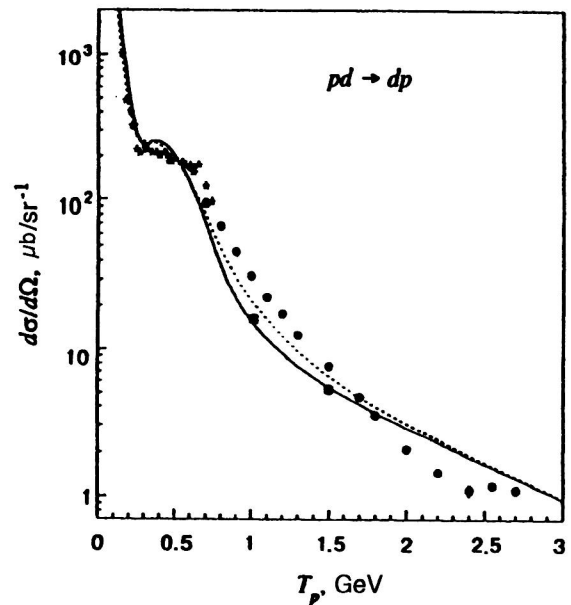


FIG. 13. Calculated cross section for the process  $pd \rightarrow dp$  at  $\theta_{c.m.} = 180^\circ$  as a function of the incident proton kinetic energy in the lab frame  $T_p$  for the NE+ $\Delta$ +SS (solid line) and NE+ $\Delta$ +SS+ $N^*$ -exchange (dashed line) mechanisms. The points are the experimental data of Refs. 20 (\*), 18 (●), and 17 (black squares).

channel, occurs for initial proton energies in the lab frame  $T_p \sim 0.2 - 0.4$  GeV. As shown in Ref. 28, the total amplitude for the exchange of positive-parity  $N^*$  isobars interferes destructively with the total amplitude for the exchange of negative-parity states. On the whole, the total contribution of  $N^*$  exchange to both the cross section and the tensor polarization in the process  $pd \rightarrow dp$  for the model of Ref. 79 is, according to Ref. 28, negligible and has practically no effect on the numerical results. According to Ref. 79, there is no interference between the  $s$  and  $p$  contributions to the inclusive reaction  $d + A \rightarrow p(0^\circ) + X$  for the NE mechanism, and this is apparently one of the reasons that  $N^*$  exchange is more important than in the process  $pd \rightarrow dp$ .

However, if the better justified angular-momentum coupling scheme (65) is used, a different result is obtained.<sup>29</sup> the interference of the  $s$  and  $p$  states is no longer destructive. As a result, the total cross section for  $n + N^*$  exchange is about 2 times higher than for pure neutron exchange in the range 0.7–1.2 GeV (Figs. 11 and 12). It is in this region that the disagreement between the predictions of the NE+ $\Delta$ +SS model and experiment is observed. As seen from Fig. 13, our calculations<sup>29</sup> using the extended NE+ $\Delta$ +SS+OBE model agree much better with the data in the range 0.7–1.5 GeV. However, the disagreement with experiment on  $t_{20}$  remains even when the OBE amplitude is included. As noted in the preceding section, this might be a consequence of the approximations made in calculating the amplitude of the  $\Delta$ -resonance mechanism.<sup>4)</sup>

**Neutron exchange and the rescattering contribution.** Numerical calculations were performed for the neutron-exchange mechanism using the deuteron wave function from the Ried soft-core (RSC) potential parametrized in Ref. 74. The parameters of the elastic  $pp$  and  $pn$  scattering ampli-

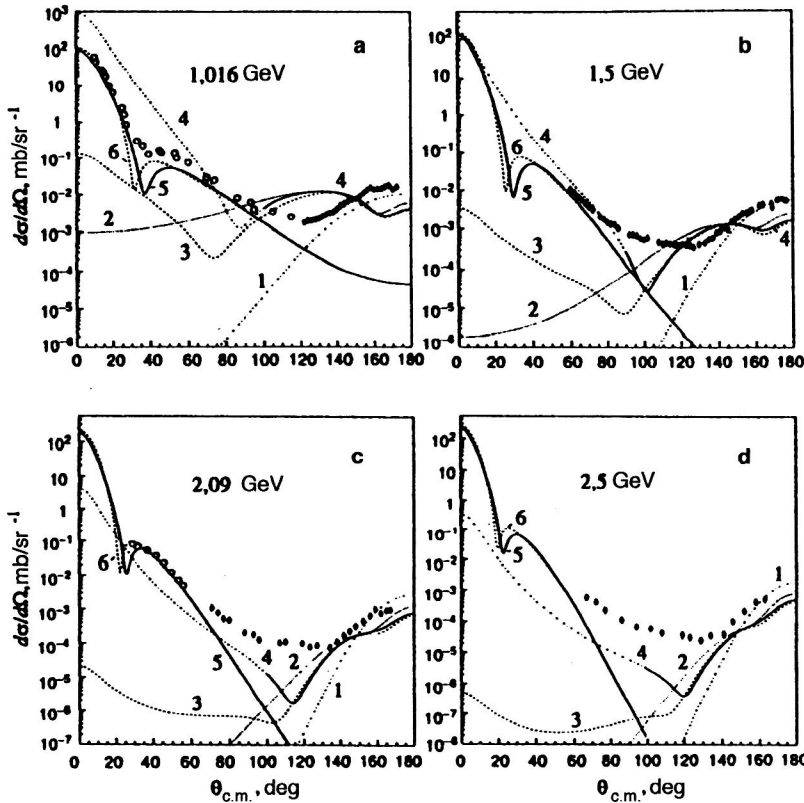


FIG. 14. Angular dependence of the cross section for elastic  $pd$  scattering in the c.m. frame at various initial proton energies: (a) 1.016 GeV; (b) 1.5 GeV; (c) 2.09 GeV; (d) 2.5 GeV. The curves were calculated using various mechanisms: (1) the NE mechanism in Fig. 10a; (2) the sum of the graphs of Figs. 10b and 10c; (3) the sum of the graphs of Figs. 10b, 10c, and 10d; (4) the sum of the graphs of Figs. 10b, 10c, 10d, and 10e; (5) the Glauber–Sitenko diffraction theory with nuclear density corresponding to the deuteron  $S$ -wave in the RSC potential; (6) the same as (5), but with Gaussian density from Ref. 89. The points are the experimental data from Refs. 16 (○) and 17 (◊).

tudes were taken from Ref. 88. In Figs. 14a–14d we show the angular dependence of the cross section for elastic  $pd$  scattering in the range  $0 \leq \theta_{c.m.} \leq 180^\circ$  at incident proton energies in the lab frame  $T_p = 1.016$  GeV, 1.5 GeV, 2.09 GeV, and 2.5 GeV. The theoretical curves were obtained using the Glauber–Sitenko theory in the forward hemisphere  $\theta_{c.m.} \leq 60^\circ$  and using the mechanism of NE with rescattering in the backward hemisphere  $\theta_{c.m.} \geq 120^\circ$ . We see from Fig. 14 that for  $T_p = 1$ –2.5 GeV and  $\theta_{c.m.} = 150$ – $180^\circ$ , the result of the Born approximation for the NE mechanism agrees satisfactorily with the experimental data in shape and absolute value. However, when  $pp$  and  $pd$  rescatterings are included, this qualitative agreement disappears. At angles  $150^\circ \leq \theta_{c.m.} < 180^\circ$  the falloff of the cross section  $d\sigma/d\Omega(\theta)$  with decreasing angle  $\theta$  is observed to slow down, in agreement with the qualitative arguments given in Sec. 3. A similar effect played an important role in the description of the angular dependence of large-angle elastic  $p^3\text{He}$  scattering using the  $np$ -pair exchange mechanism (Ref. 27).<sup>5)</sup>

The absolute value of the cross section at  $\theta_{c.m.} = 180^\circ$  decreases by a factor of  $\sim 2$ –3 in the range  $T_p = 1$ –3 GeV when distortions are included (see Fig. 15). This figure shows that the contribution of the NE mechanism including rescattering lies considerably lower than the experimental points for the cross section of  $pd$  scattering at  $\theta_{c.m.} = 180^\circ$  in the entire energy range studied, 0.5–3 GeV. The smallest deviation from experiment occurs at energies  $T_p = 2.2$ –2.4 GeV, but even here the disagreement is by a factor of  $\sim 2$ . It should be stressed that when the Paris wave function is used for the deuteron, the contribution of the NE mechanism is even smaller than when the RSC function is used (see, for example, Ref. 13). Therefore, our calculations

agree qualitatively with the conclusion of Ref. 4 regarding the role of distortions and the inadequacy of the NE mechanism for describing the absolute value of the cross section of the process  $pd \rightarrow dp$  at  $\theta_{c.m.} = 180^\circ$ . At the same time, it should be noted that the suppression due to distortions is an

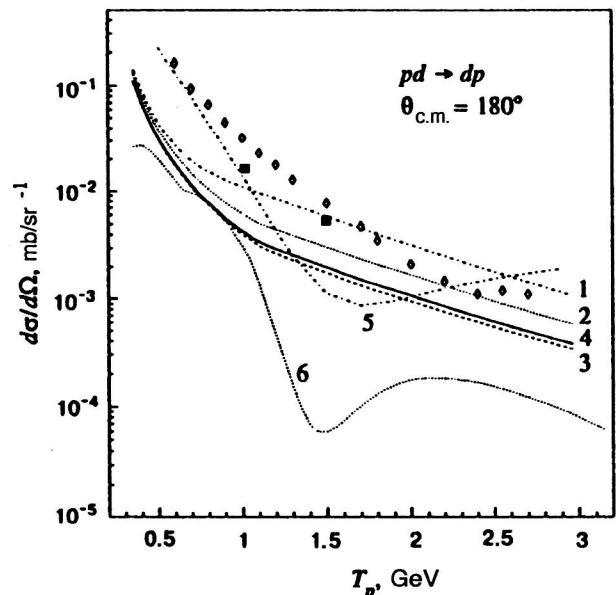


FIG. 15. Dependence of the cross section for  $pd$  scattering on the incident proton energy at  $\theta_{c.m.} = 180^\circ$ . Curves 1–4 have the same meaning as in Fig. 14; (5) is the contribution of the triangle one-pion exchange graph; (6) is for single  $pN$  scattering. The experimental data are from Refs. 18 (◊) and 17 (■).

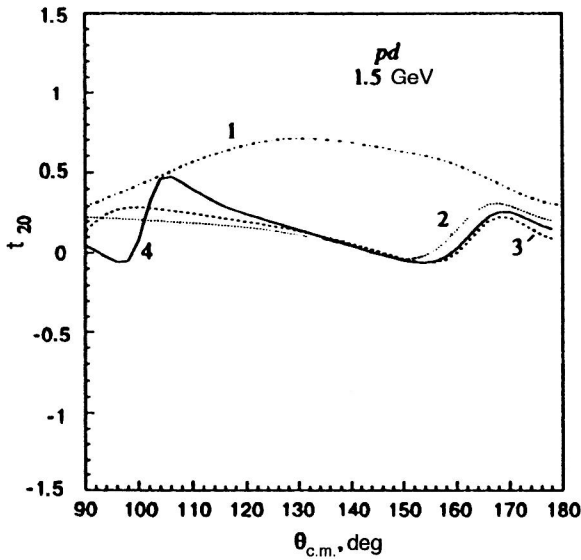


FIG. 16. Tensor polarization of the deuteron in elastic  $pd$  scattering as a function of the scattering angle at incident proton energy  $T_p = 1.5$  GeV. Curves 1–4 have the same meaning as in Fig. 14.

order of magnitude weaker than for the process  $p^3\text{He} \rightarrow ^3\text{He}p$  (Ref. 27).

The tensor polarization  $t_{20}(\theta_{\text{c.m.}})$  as a function of the scattering angle changes significantly when rescatterings are included (Fig. 16). However, at  $\theta_{\text{c.m.}} = 180^\circ$  the effect of rescatterings on  $t_{20}$  is negligible (see Fig. 17). Therefore, despite the assumptions following from the results of Ref. 24, the known discrepancy (see, for example, Ref. 26) between the predictions of the NE mechanism for  $t_{20}(\theta_{\text{c.m.}} = 180^\circ)$  and the data remains even when rescattering is included.

For comparison, in Fig. 15 we show the results of our calculations using the single-scattering and one-pion exchange (OPE) mechanisms. For the OPE mechanism we used the formalism of Ref. 90 with the parametrization of the

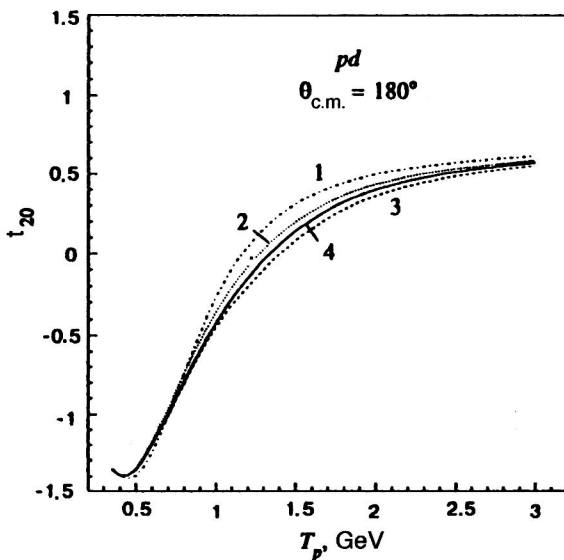


FIG. 17. Tensor polarization of the deuteron in elastic  $pd$  scattering at angle  $\theta_{\text{c.m.}} = 180^\circ$  as a function of the incident proton energy. Curves 1–4 have the same meaning as in Fig. 14.

experimental data on the reaction  $pp \rightarrow d\pi^+$  from Ref. 91. The contribution of the single-scattering mechanism was calculated in the impulse approximation using the formalism of Ref. 13 with the RSC form of the deuteron wave function. We see from Fig. 15 that the contribution of this mechanism is an order of magnitude below the experimental data in the entire energy range considered. The inclusion of double scattering as in Ref. 7 leads to additional lowering of the cross section. On the other hand, near the  $\Delta$  resonance, corresponding to proton energy  $T_p \sim 0.6$  GeV, and also at energies  $\sim 2.5$  GeV, the OPE mechanism gives a larger contribution, comparable to the experimental data. However, at energies  $\sim 1.5$  GeV the OPE contribution is almost an order of magnitude lower than the experimental points. It can be expected that the actual contribution of the OPE mechanism is even smaller owing to the absorptive nature of rescattering, which is not included in these calculations. Therefore, for energies in the range 1–2 GeV none of the mechanisms discussed here can even begin to account for the absolute value of the experimental cross section. There are apparently other mechanisms which are important, in particular, double  $pN$  scattering with excitation of  $N^*$  resonances, which is only partially included in the OPE mechanism.

## 7. THE CONTRIBUTION OF THE QUASIRESONANCE $\eta$ - $^3\text{He}$ STATE TO BACKWARD ELASTIC $pd$ SCATTERING

Analysis of the data on the  $pd \rightarrow ^3\text{He}\eta$  reaction near threshold suggests the existence of quasibound states  $B^*$  in the  $\eta$ - $^3\text{He}$  system.<sup>54,55</sup> The parameters of these states—the mass  $M_B$ , width  $\Gamma_B$ , and form factor of the transition  $\eta$   $^3\text{He} \rightarrow B^*$ , were obtained in Ref. 55 from a fit to the experimental data using the two-stage model of the reaction  $pd \rightarrow ^3\text{He}\eta$  including the final-state interaction. These results can be used to calculate the contribution of  $B^*$  states to backward elastic  $pd$  scattering.

Assuming that a quasibound state  $B^*$  is formed in the interaction of the  $\eta$  meson and the  $^3\text{He}$  nucleus produced in the process  $pd \rightarrow ^3\text{He}\eta$ , for the amplitude of the transition  $pd \rightarrow B^*$  we obtain

$$A(pd \rightarrow B^*) = \int \frac{dq^4}{(2\pi)^4} \times \frac{A_{^3\text{He}\eta \rightarrow B^*} M_a(pd \rightarrow ^3\text{He}\eta)}{2m_\eta(T_\eta - \mathbf{p}_\eta^2/2m_\eta + i\varepsilon) 2m_\tau(T_\tau - \mathbf{p}_\tau^2/2m_\tau + i\varepsilon)}; \quad (66)$$

where  $m_\tau$  and  $m_\eta$  are the masses of the  $\eta$  meson and the  $^3\text{He}$  nucleus;  $q$  is the relative 4-momentum in the  $\eta$ - $^3\text{He}$  system;  $T_i$  and  $\mathbf{p}_i$  are the kinetic energy and 3-momentum of particle (nucleus)  $i$ ;  $M_a(pd \rightarrow ^3\text{He}\eta)$  is the amplitude of the reaction  $pd \rightarrow ^3\text{He}\eta$  in the two-stage model in the notation of Ref. 55;  $A_{^3\text{He}\eta \rightarrow B^*}$  is the amplitude of the virtual process  $^3\text{He}\eta \rightarrow B^*$ , for which we have<sup>55</sup>

$$A_{^3\text{He}\eta \rightarrow B^*} = \sqrt{8\pi s_{pd}} \frac{g_0 \beta^2}{q^2 + \beta^2}; \quad (67)$$



and the parameters  $g_0$  and  $\beta$  were found in Ref. 55. The amplitude of elastic resonance  $pd$  scattering can now be written as

$$A(pd \rightarrow dp) = \frac{A(pd \rightarrow B^*)A(B^* \rightarrow dp)}{2m_{B^*}[E_k - E_0 + i\Gamma_B/2]}, \quad (68)$$

where  $E_0 = -7$  MeV is the energy of the state  $B^*$  relative to the level  $m_\eta + m_\tau$ ,  $E_k$  is the energy of the relative motion in the  $p+d$  system with relative momentum  $k$ ,  $\Gamma_B \sim 20$  MeV, and  $m_{B^*} = m_\eta + m_\tau + E_0$ .

At the maximum ( $E_k = E_0$ ), the cross section for  $pd$  scattering via the intermediate state  $B^*$  has the form

$$\frac{d\sigma}{d\Omega}(pd \rightarrow dp) = \frac{4g_0^4\beta^4}{64^2\pi^2 s_{pd}\Gamma_B^2} \frac{1}{(2\pi)^2}. \quad (69)$$

Using the values obtained in Ref. 55 for the amplitude  $M_a(pd \rightarrow {}^3\text{He}\eta)$ , from (69) we find  $d\sigma/d\Omega \sim 0.03 \mu\text{b/sr}$ , while the mechanism of one-nucleon exchange with the Paris wave function of the deuteron gives the considerably larger value<sup>13</sup>  $5 \mu\text{b/sr}$  at the same initial proton kinetic energy  $T_p \sim 1$  GeV. Therefore, the contribution of backward  $pd$  scattering via a hypothetical quasibound  $\eta$ - ${}^3\text{He}$  state is negligible.

## 8. CONCLUSION

Our analysis shows that in the process  $pd \rightarrow dp$ , in contrast to backward elastic  $p{}^3\text{He}$  scattering at energies 1–2 GeV, none of the mechanisms considered here can dominate absolutely, and the sum of all their contributions does not give a clear understanding of the nuclear structure. The process  $pd \rightarrow dp$  is therefore not as well understood theoretically as the dynamics of the process  $p{}^3\text{He} \rightarrow {}^3\text{He}p$  (Ref. 92). This is largely due to the fact that the deuteron is a very loosely bound system. Nevertheless, our analysis does lead to some constructive conclusions.

The contribution of double  $pN$  scattering with  $\Delta$ -isobar excitation is important at energies in the range 0.5–1.0 GeV. When the parameters of the  $NN \leftrightarrow N\Delta$  amplitude are correctly defined, the sum of mechanisms  $\text{NE} + \Delta + \text{SS}$  gives a qualitative description of the energy dependence of the scattering cross section in the range 0.5–1.5 GeV at  $\theta_{\text{c.m.}} = 180^\circ$ . Therefore, attempts to describe the experimental data in this energy range using only the one-nucleon exchange mechanism including the extra relativistic components of the deuteron wave function or modification of its ordinary  $pn$  component, but neglecting three-particle  $N-\Delta-N$  forces, are completely unjustified. Meanwhile, the  $\text{NE} + \Delta + \text{SS}$  model, whose parameters are most reliable near the point where the  $\Delta$  isobar goes off-shell, underestimates the absolute value of the cross section by nearly a factor of 2 in this region. It can be stated cautiously that within the 6-quark model of the deuteron we have found indications of a significant contribution from  $N^*$ -isobar exchange to the cross section for the process  $pd \rightarrow dp$  in this energy range,  $T_p \sim 0.7$ –1.2 GeV. At present it is not possible to include the contribution of other, more exotic mechanisms at these energies.

Rescatterings in the initial and final states are important. The contribution of the NE mechanism to the  $pd \rightarrow dp$  cross section at  $\theta_{\text{c.m.}} = 180^\circ$  is decreased by a factor of 2–3 by rescatterings. We have demonstrated the following qualitative effect: as the scattering angle deviates from the value  $\theta_{\text{c.m.}} = 180^\circ$ , the relative role of the nucleon exchange mechanism in the process  $p+d \rightarrow d'+p'$  grows owing to the decrease of the typical relative momenta at the  $d \rightarrow p'+n$  and  $p+n \rightarrow d'$  vertices due to rescattering.

The clearest feature of the process  $pd \rightarrow dp$  is its high sensitivity to the parameters of the form factors at the  $\pi(p)NN$  and  $\pi(p)N\Delta$  vertices. Even with the present uncertainty in the ratio of the contribution of neutron (including rescattering effects) and  $N^*$ -isobar exchange, the calculations described here allow us to state that the values of the cutoff momenta  $\Lambda_\pi \sim \Lambda_p \sim 1.3$  GeV/c widely used in the theory of the  $\pi NN$  system strongly contradict the available experimental data on the cross section for backward  $pd$  scattering in the range 0.5–1.0 GeV.

In the energy range 1–2 GeV, none of the mechanisms considered using realistic deuteron wave functions can account for the absolute value of the experimental cross section. For the NE mechanism the predictions for  $t_{20}(\theta_{\text{c.m.}} = 180^\circ)$  sharply contradict the experimental data both in the nonrelativistic approximation, and in all the relativistic approaches, and the inclusion of rescattering does not change this conclusion. Regarding this, it should be noted that according to the preliminary CEBAF data,<sup>93</sup> the tensor polarization  $t_{20}$  in elastic electron–deuteron scattering agrees qualitatively with the impulse approximation and nonrelativistic structure of the deuteron up to momentum transfer 1.35 GeV, corresponding to a typical relative momentum of the nucleons in the deuteron of  $\sim 0.6$  GeV/c. This shows that, most likely, in the process  $pd \rightarrow dp$  at energies 1–2 GeV the main role is played not by deuteron structure effects, but by mechanisms with  $N^*$ -isobar excitation, similar to the  $\Delta$  mechanism. These mechanisms must be studied theoretically just as carefully as the  $\Delta$ -resonance mechanism. However, this is much more difficult owing to the limited information available about the properties of  $N^*$  isobars. Like the  $\Delta$  mechanism,  $N^*$ -isobar mechanisms should be rather weakly sensitive to the high-momentum components of the deuteron wave function, and so they are not particularly interesting from the viewpoint of studying the relativistic structure of the deuteron. However, they may give independent information about the  $NN \leftrightarrow NN^*$  amplitudes.

The author is grateful to V. A. Karmanov, A. P. Kobushkin, V. I. Komarov, L. A. Kondratyuk, V. I. Kukulin, F. M. Lev, and V. G. Neudachin for discussions. This study was carried out with the partial support of the Russian Fund for Fundamental Research, Grant No. 96-02-17215.

<sup>1)</sup>However, as yet there is no proof that this procedure should be viewed as an exact method of constructing the electromagnetic current.

<sup>2)</sup>If we try to increase the  $\rho$ -meson contribution (while changing the  $\pi$ -exchange parameters) in (30), it is not possible to describe the data on the reaction  $pp \rightarrow pn\pi^+$  at  $T_p = 800$  MeV.

<sup>3)</sup>Naturally, here a contradiction arises between the calculated and experimental values of the deuteron quadrupole moment.

<sup>4)</sup>It should be stressed that the calculations of Refs. 28 and 29 used the version with the largest value of the oscillator parameter  $b=0.8$  F, which determines the nucleon size in the quark model and enters into the kernel of the resonating-group method.<sup>79</sup> A more realistic value is  $b=0.5-0.6$  F, for which the effective number of nucleon isobars is about a factor of three smaller.<sup>79</sup> Therefore, the results of the calculations we discuss should be viewed as an upper limit on the  $N^*$ -exchange contribution.

<sup>5)</sup>As the scattering angle  $\theta_{c.m.}$  decreases from  $100^\circ$  to  $0^\circ$ , the contribution of the NE mechanism including rescattering grows sharply, especially when  $pp$  and  $pd$  rescatterings are also included, and approaches the value predicted by the Glauber–Sitenko theory. As shown in Sec. 3, this is a consequence of the decrease of the arguments of the wave functions  $\phi_{d_i}(Q_i)$  and  $\phi_{d_f}(Q_f)$  to zero, because at angles  $\theta_{c.m.} \sim 0^\circ$  the momenta  $\mathbf{q}$  and  $\mathbf{q}'$  transferred in the rescattering are parallel to the neutron and proton momenta in the deuteron  $\mathbf{Q}_i$  and  $\mathbf{Q}_f$ , corresponding to the Born approximation of one-nucleon exchange. However, from these results we cannot make the seemingly attractive conclusion that the NE mechanism contributes significantly to forward elastic  $pd$  scattering, because the method used here to include distortions is not applicable at scattering angles  $\theta_{c.m.} \sim 0^\circ$ , just as the Glauber–Sitenko theory of multiple scattering is not applicable at angles  $\sim 180^\circ$ .

<sup>1</sup>A. K. Kerman and L. S. Kisslinger, Phys. Rev. **180**, 1483 (1969).

<sup>2</sup>N. S. Craigie and C. Wilkin, Nucl. Phys. B **14**, 477 (1969).

<sup>3</sup>V. M. Kolybasov and N. Ya. Smorodinskaya, Phys. Lett. **37B**, 272 (1971); Yad. Fiz. **17**, 1211 (1973) [Sov. J. Nucl. Phys. **17**, 630 (1973)]; A. Nakamura and L. Satta, Nucl. Phys. A **445**, 706 (1985).

<sup>4</sup>M. Levitas and J. V. Noble, Nucl. Phys. A **251**, 385 (1975).

<sup>5</sup>L. A. Kondratyuk and L. V. Shevchenko, Yad. Fiz. **29**, 792 (1979) [Sov. J. Nucl. Phys. **29**, 408 (1979)].

<sup>6</sup>V. A. Karmanov, Yad. Fiz. **29**, 1179 (1979) [Sov. J. Nucl. Phys. **29**, 607 (1979)]; **34**, 1020 (1981) [ **34**, 567 (1981)].

<sup>7</sup>S. A. Gurvitz, Phys. Rev. C **22**, 725 (1980).

<sup>8</sup>L. A. Kondratyuk, F. M. Lev, and L. V. Shevchenko, Yad. Fiz. **33**, 1208 (1981) [Sov. J. Nucl. Phys. **33**, 642 (1981)].

<sup>9</sup>B. D. Keister and J. A. Tjon, Phys. Rev. C **26**, 578 (1982).

<sup>10</sup>B. Z. Kopeliovich and F. Niedermayer, Zh. Eksp. Teor. Fiz. **87**, 1121 (1984) [Sov. Phys. JETP **60**, 640 (1984)].

<sup>11</sup>A. P. Kobushkin, J. Phys. G **12**, 487 (1986).

<sup>12</sup>A. Boudard and M. Dillig, Phys. Rev. C **31**, 302 (1985).

<sup>13</sup>O. Imambekov, Yu. N. Uzikov, and L. V. Shevchenko, Z. Phys. A **332**, 349 (1989).

<sup>14</sup>I. M. Sitnik, V. P. Ladygin, and M. P. Rekalov, Yad. Fiz. **57**, 2170 (1994) [Phys. At. Nucl. **57**, 2089 (1994)].

<sup>15</sup>M. P. Rekalov and I. M. Sitnik, Phys. Lett. B **356**, 434 (1995).

<sup>16</sup>G. W. Bennet *et al.*, Phys. Rev. Lett. **19**, 387 (1967).

<sup>17</sup>L. Dubal *et al.*, Phys. Rev. D **9**, 597 (1974).

<sup>18</sup>P. Berthet *et al.*, J. Phys. G **8**, L111 (1982).

<sup>19</sup>J. Arivieux *et al.*, Nucl. Phys. A **431**, 613 (1984).

<sup>20</sup>A. Boudard, Thesis, CEA-N-2386, Saclay (1984).

<sup>21</sup>V. Punjabi *et al.*, Phys. Lett. B **350**, 178 (1995).

<sup>22</sup>M. P. Rekalov, N. M. Piskunov, and I. M. Sitnik, Preprint E2-97-190, JINR, Dubna (1997).

<sup>23</sup>L. S. Azhgirei *et al.*, Preprint R1-97-174, JINR, Dubna (1997) [in Russian].

<sup>24</sup>A. P. Kobushkin, Preprint LANL nucl-th/9706025.

<sup>25</sup>A. G. Ableev *et al.*, Pis'ma Zh. Eksp. Teor. Fiz. **47**, 558 (1988) [JETP Lett. **47**, 649 (1988)].

<sup>26</sup>E. A. Strokovskiy, Few-Body Syst. Suppl. **8**, 186 (1995).

<sup>27</sup>L. D. Blokhintsev, A. V. Lado, and Yu. N. Uzikov, Nucl. Phys. A **597**, 487 (1996).

<sup>28</sup>Yu. N. Uzikov, Yad. Fiz. **60**, 1603 (1997) [Phys. At. Nucl. **60**, 1458 (1997)].

<sup>29</sup>Yu. N. Uzikov, in *Proceedings of the Conf. DEUTERON-97*, Dubna, 1997 [in press].

<sup>30</sup>Yu. N. Uzikov, Yad. Fiz. **55**, 2374 (1992) [Sov. J. Nucl. Phys. **55**, 1319 (1992)].

<sup>31</sup>G. I. Lykasov, Fiz. Élem. Chastits At. Yadra **24**, 140 (1993) [Phys. Part. Nuclei **24**, 59 (1993)].

<sup>32</sup>B. A. Karmanov, Fiz. Élem. Chastits At. Yadra **19**, 525 (1988) [Sov. J. Part. Nucl. **19**, 228 (1988)]; J. Carbonell, B. Desplanques, V. A. Karmanov, and J.-F. Mathiot, Phys. Rep. **300**, 215 (1998).

<sup>33</sup>S. M. Dorkin, L. P. Kaptari, and S. S. Semykh, Preprint R-96-407, JINR, Dubna (1996) [in Russian].

<sup>34</sup>L. P. Kaptari, B. Kämpfer, S. M. Dorkin, and S. S. Semikh, Phys. Lett. B **404**, 8 (1997).

<sup>35</sup>L. P. Kaptari, B. Kämpfer, S. M. Dorkin, and S. S. Semikh, Preprint LANL nucl-th/9709071.

<sup>36</sup>B. L. G. Bakker, L. A. Kondratyuk, and M. V. Terentjev, Nucl. Phys. B **158**, 497 (1979).

<sup>37</sup>F. M. Lev, Fiz. Élem. Chastits At. Yadra **21**, 1251 (1990) [Sov. J. Part. Nucl. **21**, 534 (1990)]; *Some Problems in the Relativistic Quantum Mechanics of Systems With a Given Number of Degrees of Freedom* [in Russian] (Dubna, 1988).

<sup>38</sup>P. L. Chung, F. Coester, B. D. Keister, and W. N. Polyzou, Phys. Rev. C **37**, 2000 (1988).

<sup>39</sup>F. Coester and W. N. Polyzou, Phys. Rev. D **26**, 1348 (1982).

<sup>40</sup>S. N. Sokolov, Teor. Mat. Fiz. **36**, 193 (1978) [Theor. Math. Phys. (USSR) ].

<sup>41</sup>S. N. Sokolov and A. N. Shatnii, Teor. Mat. Fiz. **37**, 291 (1978) [Theor. Math. Phys. (USSR) ].

<sup>42</sup>P. A. M. Dirac, Rev. Mod. Phys. **21**, 392 (1949).

<sup>43</sup>V. A. Karmanov and A. V. Smirnov, Nucl. Phys. A **575**, 520 (1994).

<sup>44</sup>B. Desplanques, V. A. Karmanov, I.-F. Mathiot, Nucl. Phys. A **589** 697 (1995).

<sup>45</sup>F. M. Lev, Ann. Phys. (N.Y.) **237**, 355 (1995).

<sup>46</sup>M. A. Braun and M. V. Tokarev, Fiz. Élem. Chastits At. Yadra **22**, 1237 (1991) [Sov. J. Part. Nucl. **22**, 601 (1991)].

<sup>47</sup>V. P. Ladygin and N. B. Ladygina, Preprint E2-96-322, JINR, Dubna (1996).

<sup>48</sup>M. V. Tokarev, in *Proceedings of the Eleventh Seminar on High Energy Physics Problems*, edited by A. M. Baldin and V. V. Burov, Dubna, 1994, p. 456.

<sup>49</sup>G. A. Leksins, Zh. Éksp. Teor. Fiz. **32**, 445 (1957) [Sov. Phys. JETP **5**, 378 (1957)]; G. W. Bennet *et al.*, Phys. Rev. Lett. **19**, 387 (1967); N. E. Booth *et al.*, Phys. Rev. D **4**, 1261 (1971); B. F. Bonner *et al.*, Phys. Rev. Lett. **39**, 1253 (1977); V. I. Komarov *et al.*, Yad. Fiz. **16**, 234 (1972) [Sov. J. Nucl. Phys. **16**, 129 (1972)].

<sup>50</sup>G. W. Barry, Ann. Phys. (N.Y.) **73**, 482 (1972); L. Vegh, Preprint E2-12369, JINR, Dubna (1979).

<sup>51</sup>L. A. Kondratyuk, F. M. Lev, and L. V. Shevchenko, Preprint 120, ITEP, Moscow (1980); L. A. Kondratyuk and L. V. Shevchenko, in *Proceedings of the Sixteenth Winter School of the LIYaF* [in Russian], Leningrad, 1981, p. 115.

<sup>52</sup>L. A. Kondratyuk and L. V. Shevchenko, Preprint 152, ITEP, Moscow (1984).

<sup>53</sup>L. A. Kondratyuk, in *Proceedings of the Symp. on Nucleon–Nucleon and Hadron–Nucleus Interactions at Intermediate Energies* [in Russian], Leningrad, 1984, p. 402.

<sup>54</sup>C. Wilkin, Phys. Rev. C **47**, R938 (1993).

<sup>55</sup>L. A. Kondratyuk, A. V. Lado, and Yu. N. Uzikov, Yad. Fiz. **58**, 524 (1995) [Phys. At. Nucl. **58**, 473 (1995)].

<sup>56</sup>L. A. Kondratyuk and F. M. Lev, Yad. Fiz. **26**, 294 (1977) [Sov. J. Nucl. Phys. **26**, 153 (1977)].

<sup>57</sup>O. Imambekov and Yu. N. Uzikov, Yad. Fiz. **47**, 1089 (1988) [Sov. J. Nucl. Phys. **47**, 695 (1988)].

<sup>58</sup>T.-S. H. Lee and A. Matsuyama, Phys. Rev. C **32**, 516 (1985).

<sup>59</sup>T.-S. H. Lee, Phys. Rev. C **29**, 195 (1984).

<sup>60</sup>A. Matsuyama and T.-S. H. Lee, Phys. Rev. C **34**, 1900 (1986).

<sup>61</sup>J. Dubach *et al.*, Phys. Rev. C **34**, 944 (1986); G. H. Lamot *et al.*, Phys. Rev. C **35**, 239 (1987).

<sup>62</sup>J. Hudomaly-Gabitzsch *et al.*, Phys. Rev. C **18**, 2666 (1978).

<sup>63</sup>A. D. Hancock *et al.*, Phys. Rev. C **27**, 2742 (1983).

<sup>64</sup>B. J. Verwest, Phys. Lett. **83B**, 161 (1979).

<sup>65</sup>P. Fernandez de Cordoba, E. Oset, M. J. Vicente-Vacas *et al.*, Nucl. Phys. A **586**, 586 (1995).

<sup>66</sup>A. Engle, Nucl. Phys. A **603**, 387 (1996).

<sup>67</sup>M. Gari and U. Kaulfuss, Phys. Lett. **136B**, 139 (1984).

<sup>68</sup>T. D. Cohen, Phys. Rev. D **34**, 2187 (1986).

<sup>69</sup>V. Dmitriev, O. Sushkov, and C. Gaarde, Nucl. Phys. A **459**, 503 (1986).

<sup>70</sup>O. Imambekov, Yu. N. Uzikov, and L. V. Shevchenko, Yad. Fiz. **44**, 1459 (1986) [Sov. J. Nucl. Phys. **44**, 950 (1986)].

- <sup>71</sup>O. Imambekov and Yu. N. Uzikov, *Yad. Fiz.* **52**, 1361 (1990) [*Sov. J. Nucl. Phys.* **52**, 862 (1990)].
- <sup>72</sup>J. A. Tejedor, PhD Thesis, Valencia University (1995).
- <sup>73</sup>M. Lacombe, B. Loiseau, R. Vinh Mau *et al.*, *Phys. Lett.* **101B**, 139 (1981).
- <sup>74</sup>G. Alberi, L. P. Rosa, and Z. D. Tome, *Phys. Rev. Lett.* **34**, 503 (1975).
- <sup>75</sup>V. M. Krasnopolsky, V. I. Kukulin, V. N. Pomerantsev, and P. B. Sazonov, *Phys. Lett.* **165B**, 7 (1985).
- <sup>76</sup>L. A. Kondratyuk and F. M. Lev, Preprint 147, ITEP, Moscow (1977) [in Russian].
- <sup>77</sup>O. Imambekov and Yu. N. Uzikov, *Izv. Akad. Nauk SSSR, Ser. Fiz.* **51**, 947 (1987) [*Bull. Acad. Sci. USSR, Phys. Ser.* ].
- <sup>78</sup>Yu. N. Uzikov, *Yad. Fiz.* **60**, 1603 (1997) [*Phys. At. Nucl.* **60**, 1458 (1997)].
- <sup>79</sup>A. P. Kobushkin, A. I. Syamtonov, and L. Ya. Glozman, *Yad. Fiz.* **59**, 833 (1996) [*Phys. At. Nucl.* **59**, 795 (1996)].
- <sup>80</sup>H. Melosh, *Phys. Rev. D* **9**, 1095 (1974).
- <sup>81</sup>A. G. Sitenko, *Fiz. Elem. Chastits At. Yadra* **4**, 546 (1973) [*Sov. J. Part. Nucl.* **4**, 231 (1973)].
- <sup>82</sup>G. D. Alkhazov, V. V. Anisovich, and P. É. Volkovitskiĭ, *Diffraction Interaction of Hadrons With Nuclei at High Energies* [in Russian] (Nauka, Leningrad, 1991).
- <sup>83</sup>L. S. Sharma, Y. S. Bhasin, and A. N. Mitra, *Nucl. Phys. B* **35**, 466 (1971); J. S. Sharma and A. N. Mitra, *Phys. Rev. D* **9**, 2547 (1974).
- <sup>84</sup>V. G. Neudatchin, I. T. Obukhovskiy, V. I. Kukulin, and N. F. Golovanova, *Phys. Rev. C* **11**, 128 (1975).
- <sup>85</sup>A. Faessler, F. Fernandez, G. Lübeck, and K. Shimizu, *Nucl. Phys. A* **402**, 555 (1983).
- <sup>86</sup>A. M. Kusainov, V. G. Neudatchin, and I. T. Obukhovskiy, *Phys. Rev. C* **44**, 2343 (1991); L. Ya. Glozman, V. G. Neudatchin, and I. T. Obukhovskiy, *Phys. Rev. C* **48**, 389 (1993).
- <sup>87</sup>L. Ya. Glozman and E. I. Kuchina, *Phys. Rev. C* **49**, 1149 (1994).
- <sup>88</sup>Particle Data Group Report UCRL 20000 NN.1979.
- <sup>89</sup>V. G. Neudachin, V. I. Kukulin, and A. Sakharuk, *Yad. Fiz.* **52**, 738 (1993) [*Phys. At. Nucl.* **52**, 473 (1993)].
- <sup>90</sup>L. Vegh, *J. Phys. G* **8**, L121 (1979).
- <sup>91</sup>G. Fäldt and C. Wilkin, *Phys. Lett. B* **354**, 20 (1995).
- <sup>92</sup>Yu. N. Uzikov, *Fiz. Elem. Chastits At. Yadra* **29**, No. 4 (1998) [*Phys. Part. Nuclei* **29**, No. 4 (1998)].
- <sup>93</sup>S. Kox, in *Proceedings of the Intern. Conf. on Electromagnetic Interactions of Nucleons and Nuclei*, Santorini, Greece, 1997.

Translated by Patricia A. Millard